AD-A207 323

OFFICE OF NAVAL RESEARCH

Contract N00014-82-K-0576

Technical Report No. 41

ADSORPTION AND COADSORPTION OF CO AND NO ON THE RH(100) SURFACE: A THEORETICAL ANALYSIS

by

D. Lj. Vuckovic, S. A. Jansen and R. Hoffmann

Department of Chemistry
Cornell University
Baker Laboratory
Ithaca, NY 14853-1301

April 1989

Reproduction in whole or in part is permitted
for any purpose of the United States Government

This document has been approved for public release
and sale; its distribution is unlimited

DTIC
ELECTE
MAY 01 1989
S D
E

89 051

SECURITY CLASSIFICATION OF THIS PAGE

REPORT DOCUMENTATION PAGE

1a. REPORT SECURITY CLASSIFICATION unclassified	1b. RESTRICTIVE MARKINGS
2a. SECURITY CLASSIFICATION AUTHORITY	3. DISTRIBUTION / AVAILABILITY OF REPORT
2b. DECLASSIFICATION / DOWNGRADING SCHEDULE	
4. PERFORMING ORGANIZATION REPORT NUMBER(S) #41	5. MONITORING ORGANIZATION REPORT NUMBER(S)
6a. NAME OF PERFORMING ORGANIZATION Department of Chemistry 6b. OFFICE SYMBOL (If applicable)	7a. NAME OF MONITORING ORGANIZATION ONR
6c. ADDRESS (City, State, and ZIP Code) Cornell University Baker Laboratory Ithaca, NY 14853-1301	7b. ADDRESS (City, State, and ZIP Code) 800 Quincy Street, Arlington
8a. NAME OF FUNDING / SPONSORING ORGANIZATION 8b. OFFICE SYMBOL (If applicable)	9. PROCUREMENT INSTRUMENT IDENTIFICATION NUMBER Report #41
8c. ADDRESS (City, State, and ZIP Code)	10. SOURCE OF FUNDING NUMBERS PROGRAM ELEMENT NO. / PROJECT NO. / TASK NO. / WORK UNIT ACCESSION NO.

11. TITLE (Include Security Classification)

Adsorption and Coadsorption of CO and NO on the Rh(100)Surface: A Theoretical Analysis

12. PERSONAL AUTHOR(S)
D. Lj. Vuckovic, S. A. Jansen and R. Hoffmann

13a. TYPE OF REPORT	13b. TIME COVERED	14. DATE OF REPORT (Year, Month, Day)	15. PAGE COUNT
Technical Report #41	FROM _____ TO _____	April 14, 1989	

16. SUPPLEMENTARY NOTATION

17. COSATI CODES			18. SUBJECT TERMS (Continue on reverse if necessary and identify by block number)
FIELD	GROUP	SUB-GROUP	
			Carbon monoxide, Nitric oxide, Carbon dioxide, Diatomic Nitrogen

19. ABSTRACT (Continue on reverse if necessary and identify by block number)

The adsorption of CO, NO and their coadsorption on the Rh(100) surface are discussed in terms of extended Hückel/tight binding calculations. Experimentally, it is not easy to resolve the linear and bent forms of NO and for this reason our calculations serve to examine not only the proposed adsorption geometries but also as means to investigate the NO dissociation mechanism. This dissociation is believed to be the fundamental step in the CO/NO reaction. The adsorption site and geometry are discussed for several NO chemisorptions. In addition, a discussion of the CO/NO reaction for the proposed adsorption of NO is presented. From this analysis, it is clear that predissociation of NO into atomic components can lead to recombination producing the desired reaction products, CO_2 and N_2. Furthermore, the coadsorbate interactions can lead directly to the desired products.

20. DISTRIBUTION / AVAILABILITY OF ABSTRACT ☒ UNCLASSIFIED/UNLIMITED ☐ SAME AS RPT. ☐ DTIC USERS	21. ABSTRACT SECURITY CLASSIFICATION unclassified
22a. NAME OF RESPONSIBLE INDIVIDUAL Roald Hoffmann	22b. TELEPHONE (Include Area Code) 607-255-3419 22c. OFFICE SYMBOL

DD FORM 1473, 84 MAR 83 APR edition may be used until exhausted. All other editions are obsolete.

SECURITY CLASSIFICATION OF THIS PAGE

Adsorption and Coadsorption of CO and NO on the Rh(100) Surface: A Theoretical Analysis

Dragan Lj. Vučković[a], Susan A. Jansen and Roald Hoffmann*
Department of Chemistry and Materials Science Center
Cornell Unversity, Ithaca, NY 14853-1301

Abstract:

The adsorption of CO, NO and their coadsorption on the Rh(100) surface are discussed in terms of extended Hückel/tight binding calculations. Experimentally, it is not easy to resolve the linear and bent forms of NO and for this reason our calculations serve to examine not only the proposed adsorption geometries but also as means to investigate the NO dissociation mechanism. This dissociation is believed to be the fundamental step in the CO/NO reaction. The adsorption site and geometry are discussed for several NO chemisorptions. In addition, a discussion of the CO/NO reaction for the proposed adsorption of NO is presented. From this analysis, it is clear that predissociation of NO into atomic components can lead to recombination producing the desired reaction products, CO_2 and N_2. Furthermore, the coadsorbate interactions can lead directly to the desired products.

ssion For
GRA&I
TAB
nounced
ification
Distribution/
Availability Codes
Dist | Avail and/or Special
A-1

[a]Permanent address: The Boris Kidric Institute of Nuclear Sciences, Vinca, Department of Chemistry 050, 11001 Belgrade, Yugoslavia.

DTIC COPY INSPECTED 6

The catalytic reduction of nitric oxide with carbon monoxide over transition metal surfaces, forming CO_2 and N_2 as reaction products, is important in pollution abatement. Among the transition metals, rhodium is the most effective catalyst for this purpose, and in the automotive exhaust environment it is the only catalyst which works effectively to reduce NO. Details of the catalytic mechanism are still unclear. In this work, we will study theoretically the coadsorption of CO and NO on the Rh(100) surface, as well as the behavior of each individual adsorbate.

Let us first review briefly some previous experimental and theoretical work in this area. The adsorption of CO on transition metal surfaces has been studied extensively[1-10]. The experimental work has been accompanied by much theoretical consideration[11-16]. On early transition metals CO chemisorbs dissociatively, and on late transition metals, molecularly[1,12]. On most rhodium surfaces, CO is adsorbed molecularly with the carbon end down. The adsorption geometries and site preferences for low index Rh surfaces are well known[3-6]. At lower coverages, the only CO state present is a molecular species in an on-top site, i.e. each CO being bound to a single Rh surface atom. With increasing CO coverage, a new compressed surface pattern is formed, with some CO starting to occupy two-fold bridging sites[3-6,17]. The simplest general picture of CO chemisorption postulates electron donation from the CO 5σ (HOMO) orbital into suitable transition metal d orbitals and back donation from the surface d orbitals into CO $2\pi^*$ (LUMO) orbitals. This is usually referred to as the Blyholder model[18]. There

is some evidence that this simple picture may not be complete. Other CO orbitals may be important, especially the 4σ[16,19]. For a previous theoretical study of the CO chemisorption on transition metal surfaces in this group see ref. 12.

Nitric oxide chemisorption on transition metal surfaces has also been studied extensively[1,4,5,8,20-25]. It is much more complex and not as well understood as CO chemisorption. The NO ligand in both discrete complexes and on surfaces appears to have the freedom to bond linearly or bent. In nitrosyl transition metal complexes, the extremes can be represented as $M-(NO)^+$, or $M-(NO)^-$, with the first leading to a linearly bonded and the latter to a bent NO configuration (NO axis being substantially tilted away from the surface normal)[25-29]. In general, NO undergoes dissociative chemisorption more readily than CO. For NO on group VIII metals there is evidence for low temperature dissociative adsorption, as well as molecular adsorption in a variety of geometries, including a bent form, a bridged form and a linear form[30]. However, unambiguous evidence for bent forms is difficult to obtain because of the complexity of the NO spectra.

The adsorption and decomposition of nitric oxide on rhodium has received some attention in the literature[2,4,5,20,23,25,31,32]. Both molecular and dissociative chemisorption is found, with the latter leading eventually to O_2 and N_2 desorption. Just to illustrate the complexity of NO adsorption on Rh surfaces, it is worthwhile to mention that Dubois et al.[5] have reported at least five different NO species

on Rh(111) using high resolution EELS. For a detailed theoretical study of NO on Ni(111), see another contribution from this group[33].

The CO/NO reaction on the transition metals has been investigated, for instance,on clean polycrystalline Pt[34], Pt(111)[35], Pt(100)[8] and Ru(001)[36]. In general, it is accepted that the NO dissociation is a prerequisite for the reaction to occur, at least for some surfaces. On surfaces such as Pt(111), in which NO is adsorbed only molecularly, no reaction with CO occurs[34,35].

The mechanism of nitric oxide reduction is unclear and despite its significance there have been relatively few mechanistic studies examining the CO/NO process on well defined rhodium surfaces. The few that exist are recent: Rh(110)[4], Rh(331)[5], polycrystalline Rh[37], Rh(111)[38] and Rh(100)[39]. There have been numerous investigations of the CO/NO reaction over supported rhodium such as Rh/Al_2O_3[20,40] and Rh/SiO_2[41]. The basic question about the reaction mechanism is whether the major steps involve NO decompositon, or if it is a true bimolecular reaction between adsorbed CO and NO. For the Rh(111) surface, it wasrecently shown[38d] that the mechanism goes exclusively through the NO decomposition step.

In an attempt to shed some light on NO adsorption and its coadsorption and reaction with CO we present here the theoretical investigation of the CO/NO system on a Rh(100) surface, using the extended Hückel/tight binding method[42]. This procedure has well-known deficiencies but in general describes simply the reactive trends responsible for surface chemistry.

Clean Rh(100)

The Rh(100) single crystal surface is well defined and nonreconstructed[2,31,39,43], giving a sharp (1x1) LEED pattern. For this reason, the model chosen for the calculation was a three layer two dimensional slab of the fcc rhodium metal structure[44] with lattice constant of 3.8032A and nearest neighbor separations of 2.6893A (1). Whether the use of the three layer slab model to represent the surface in our calculation is appropriate has, been discussed earlier[12,33,45,46].

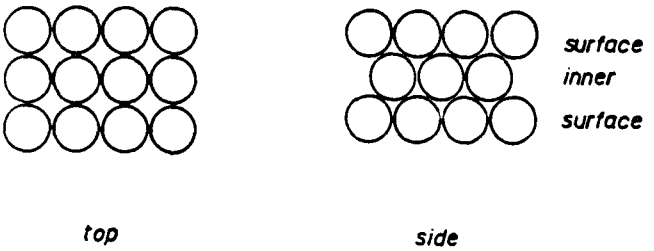

1

The calculated density of states for a three layer slab shows a d band between -7.0 and -13.0 eV, and dispersed s and p bands starting from -12.0 eV and up to 20 eV. The Fermi level is at 8.55 eV (Figure 1a). Since the surface atoms have a lower coordination number than the bulk atoms, their states are less dispersed than the bulk states. If the Fermi level falls above the midpoint of the d block, as it does for rhodium, then the

surface should have a negative charge with respect to the bulk[46]. In our case, the total charge on the surface rhodium atom is an exaggerated 9.32 electrons and the bulk atom have a total of 8.35 electrons.

CO on the Rh(100) Surface

CO readily chemisorbs on the Rh(100) surface with a sticking coefficient near unity. The chemisorption is molecular and no evidence for dissociation was observed, as for all late transition metal surfaces[1]. On the Rh(100) surface, CO site preference is coverage and temperature dependent[2,47]. It is necessary to adsorb CO gas at 25°C or below to obtain well-ordered surface structures, with disordering temperature about 125°C. At lower exposures, a c(2x2) adsorption LEED pattern was observed and at higher exposures above 1 L this structure is compressed into a hexagonal overlayer, which is a split (2x1) pattern. The saturation coverage is about $\Theta = 0.82$. At lower temperatures (~100 K) some other complicated structures were observed[47] similar to the coincidence lattice pattern reported by Tucker[48], with a rectangular unit cell which is 4x1 times the Rh face-centered cell. This result was later questioned by Castner et al.[2] since it was unclear whether these studies were carried out on an initially clean surface. Kim et al.[47a] have found a similar compressed structure.

In general, we can say that at lower exposure a regular c(2x2) pattern (coverage of 0.5) is observed with the on-top

adsorption geometry. Higher exposures lead to a compressed LEED structure with a saturation coverage near 0.8, involving a new adsorption state with a higher coordination number. This can be assigned to a two-fold bridging state[39]. The difference of the heats of desorption between these two states was calculated by Hendershot and Hansen[39] to be 3.2 kcal/mol.

The molecular orbitals of an isolated CO are well known[49]. The highest occupied molecular orbital (HOMO) is mainly the carbon lone pair 5σ (2a), and its energy is lower than the d states of most metals. In the generally accepted picture of CO chemisorption, 5σ is stabilized through interaction with surface d states relative to other CO levels. The lowest unoccupied molecular orbital (LUMO) of the free CO molecule the $2\pi^*$ consists of two antibonding combinations (2b) with larger coefficients on the carbon atom. As we have already

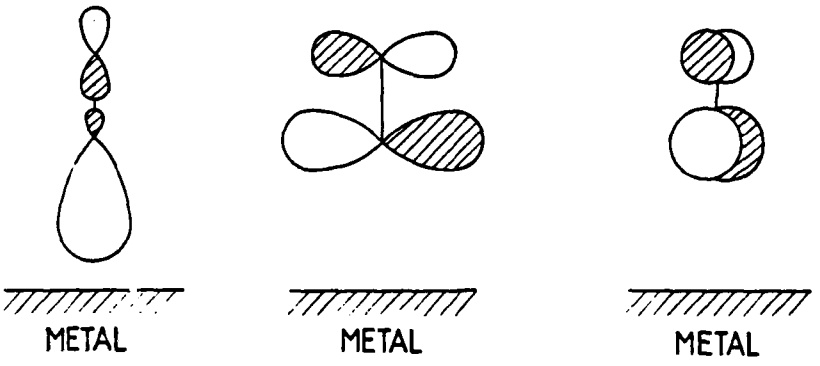

a b

2

mentioned, these two orbitals are mainly involved in the chemisorption mechanism (Blyholder model). Upon chemisorption the $2\pi^*$ derived orbitals are partially filled and consequently,

the CO bond is weakened. Aside from the frontier orbitals, other CO orbitals are usually not taken into account because they are too distant in energy from the active states of the surface.

The band structure of an isolated CO overlayer can be found in a previous contribution from our group on CO bonding to metal surfaces[12], as well as in the work of others. We will focus our attention on the coverage and site dependence of CO chemisorbed on Rh(100). The results of our calculations are summarized in Table 1. We have considered two adsorption geometries, on-top (3) and two-fold bridging (4), although it is known that an on top adsorption is strongly preferred for lower coverages on the Rh(100) surface. The coverage dependence

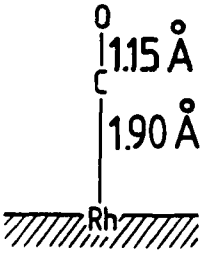

3

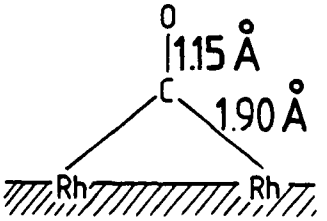

4

analysis was carried out for each adsorption geometry with three different coverages of the surface of 1, 1/2 and 1/4 which is represented by a top view in 5, 6 and 7, respectively. Table 1 however reports the results for one coverage, c(2x2) and Θ=0.5, because the results for other coverages are so similar.

Table 1. Some Bonding Characteristics for c(2x2)CO on a Model Rh(100) Slab, θ= 0.5.

		Free CO	On-top	Bridging
CO Electron Densities	4σ	2	1.78	1.72
	$1\pi_x$	2	1.99	1.98
	$1\pi_y$	2	1.99	1.95
	5σ	2	1.67	1.69
	$2\pi_x$	0	0.38	0.46
	$2\pi_y$	0	0.38	0.76
Overlap Populations	C-Rh	-	0.87	0.62
	C-O	1.44	1.23	1.09
Binding Energy (eV)[a]		-	2.48	3.07

[a] Binding energy defined as $(E_{CO} + E_{Rh(100)}) - E_{CO+Rh(100)}$.

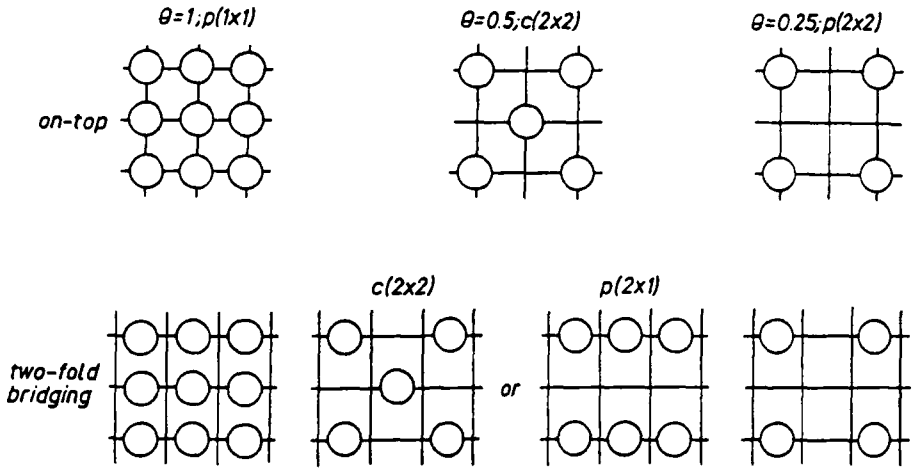

5 6 7

Note the forward donation in the depopulation of the 5σ (and 4σ) and the back donation in the population of the $2\pi^*$. In the bridging mode the degeneracy of the π orbitals is, of course, lost; the greater back donation is to the π orbital in the Rh-C-Rh plane, which is able to interact in σ fashion with the Rh orbitals. With that greater back donation, there comes a greater weakening of the C-O bond. The binding energies cannot be relied on, because we assume and cannot optimize a Rh-C distance. Not much changes for other coverages, except that the binding energy, by its decrease, clearly shows that the CO's are uncomfortable compressed at $\theta = 1.0$.

Let's look with a little more detail at the interactions in the on-top c(2x2)CO+Rh(100) system. At left in Figure 1 is

Figure 1 here

the DOS (density of states) of a naked Rh(100) slab (Fig. 1a), in the center(Fig. 1b) the composite surface plus CO overlayer, and at right(Fig. 1c) the energy levels of an isolated CO molecule. The density of states curve clearly shows that the major surface-adsorbate interactions involve 5σ and $2\pi^*$ CO orbitals, although the 4σ orbital is also shifted toward lower energies. The metal-CO 5σ interaction is mainly accomplished through electron donation to appropriate surface orbitals, i.e. d_{z^2} which are pointed directly toward the 5σ and 4σ orbitals (8). The net result is depopulation of the 5σ and 4σ from the 2 electrons each carry for a free CO molecule, to 1.67 and 1.78 electrons, respectively, in the composite system (Table 1). As a result of this the 5σ and 4σ are pushed down in energy (Figure 2a). The d_{z^2} orbitals are pushed up and consequently a greater portion of the

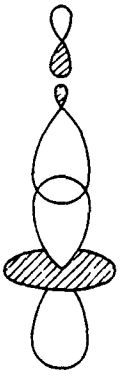

8

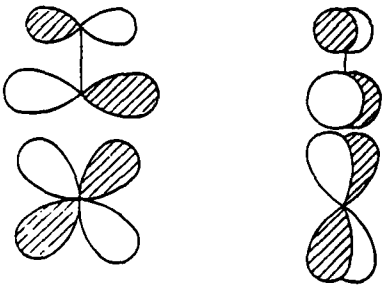

9

d_{z^2} band is raised above the Fermi level. Another very strong

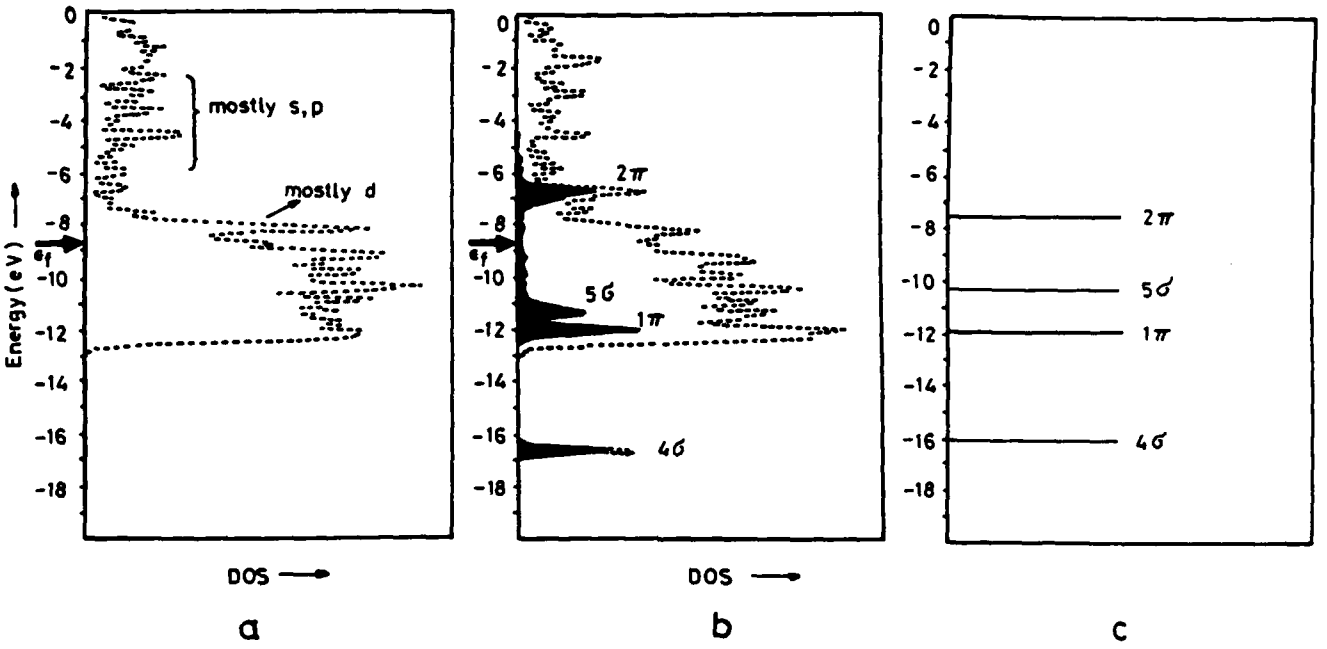

Figure 1. (a) Total DOS of the three layer slab, with Fermi level (ϵ_f) and s, p and d bands indicated; (b) Total DOS of the c(2x2)CO-Rh(100) system (broken line) and projected DOS of adsorbed CO molecule (black areas); (c) Energy levels of an isolated CO molecule.

metal-adsorbate interaction is through the CO $2\pi^*$ orbitals interaction with the surface d_π orbitals ($d_{xz,yz}$), as represented schematically in 9. The initially empty $2\pi^*$ orbitals are now partly populated in the composite CO+Rh(100) system, with an electron density of 0.76 electrons, while the corresponding surface d_π states are depopulated .

Figures 2,3 here

Another way to follow the involvement of the various orbitals in bond formation is through the crystal orbital overlap population (COOP) analysis[50]. The COOP curve really represents an overlap population weighted density of states. It weights the states in each energy interval by their contribution to the overlap population. Such a COOP curve for C-O and C-Rh bonding in our c(2x2)CO+Rh(100) system is presented in Figure 3. The main CO orbital contributions are marked and we can see that the $2\pi^*$ orbitals (i.e. their bonding combination with the d_π) are C-Rh bonding and C-O antibonding. The CO 1π orbitals are still the major bonding CO orbitals. The 5σ is both C-O and C-Rh bonding, but its absolute contribution to these bonds is small. On the other hand, the COOP curve shows that the 4σ makes a major contribution to C-Rh bonding.

What is the reason for large involvement of the 4σ? One thinks 4σ is an oxygen based lone pair, 5σ is on carbon. Actually both are quite delocalized, and Table 2 shows their composition for free CO with our parameters. Unfortunately, the make-up of these orbitals is somewhat parameter dependent. One can see the delocalization in both.

Table 2. The wave function coefficients of free CO 4σ and 5σ molecular orbitals with our parameters (see Appendix).

		4σ	5σ
C	(s)	-0.7197	0.3308
	(P_x)	0.0000	0.0000
	(P_y)	0.0000	0.0000
	(P_z)	0.4051	-0.4874
O	(s)	0.2949	0.1147
	(P_x)	0.0000	0.0000
	(P_y)	0.0000	0.0000
	(P_z)	0.4362	0.7768

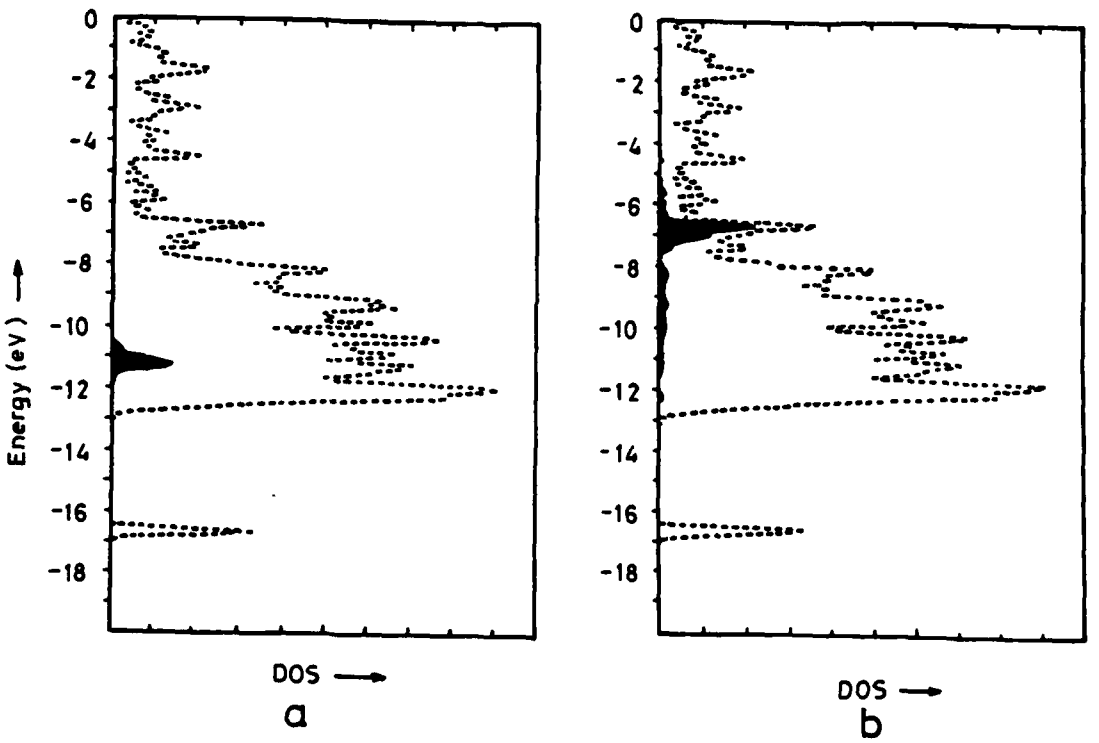

Figure 2. Projected DOS (black areas) of 5σ (a) and 2π (b) CO orbitals in a c(2x2)CO-Rh(100) system. Broken lines represent the total DOS of the system. The peak between -16 and -17eV is mainly CO 4σ.

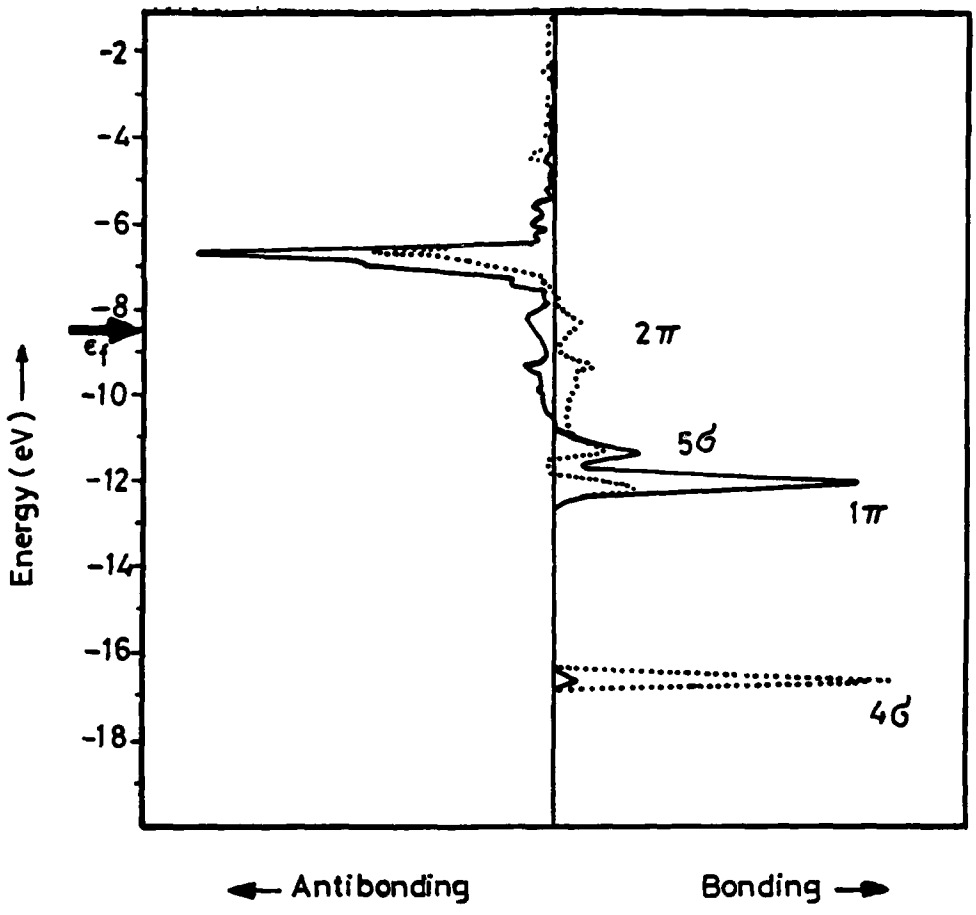

Figure 3. Crystal Orbital Overlap Population (COOP) curve for an on-top c(2x2)CO-Rh(100) system. Full line: carbon-oxygen bond; dotted line: rhodium-carbon bonding.

Really what matters is the overlap these orbitals have with another group. With the parameters we have used, a probe H is orbital placed at a distance 1.0 - 2.0 A away from the carbon end of CO actally has a bigger overlap with 4σ than 5σ. Still its net interaction with 4σ, though substantial, is less than with 5σ because 5σ is closer in energy to the hydrogen (or the frontier orbitals of a metal).

The CO 4σ orbital contribution to chemisorption in the present study might be overestimated by the use of charge iterated parameters for carbon and oxygen atoms in CO overlayer on the rhodium surface (see Appendix). But even with the use of standard carbon and oxygen parameters in extended Hückel molecular calculations[51] we had almost the same effect as here. We note here also that others have suggested a significant role for the 4σ orbital[19a,f].

CO Bridging Site

We consider the bridging geometry in some detail not because it is favored for CO on Rh(100), but because of the possibility that such a state may be involved in the coadsorption pattern with NO.

Our results for an adsorption geometry presented in 4 and for a c(2x2) LEED pattern (lower left part in 6) are also presented in Table 1. We have chosen the same C-Rh distance although it is known that bridge-bonded species should have somewhat longer distances.

The bonding here is a little bit more complicated. The CO

$2\pi^*$ and 5σ orbitals still interact with the surface d_{z^2} orbitals but less effectively. The corresponding bonding combinations are shown in 10 and 11. In addition, both CO frontier orbitals can

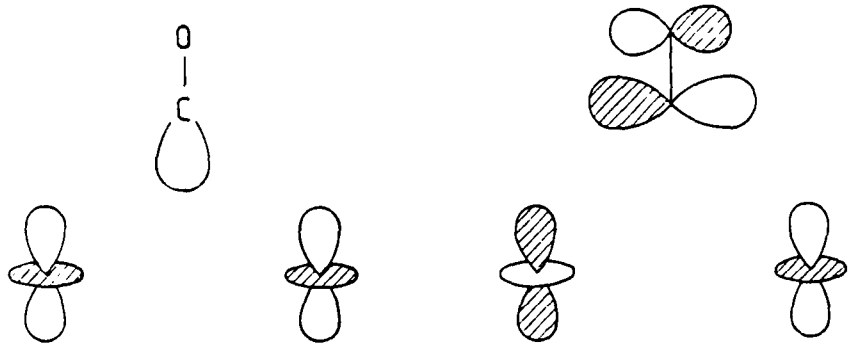

10 11

interact even more efficiently with the surface $d_{xz,yz}$ orbitals; the bonding combinations are shown in 12 and 13. The $2\pi^*$ orbitals interact with surface antibonding $d_{xz,yz}$ orbitals (13), that is with the upper part of the d band. Since the $2\pi^*$ energy falls just at that energy, the interaction is quite efficient. Thus the filling of the CO $2\pi^*$ orbitals is higher in the bridging that in the on-top geometry (Table 1). Consequently, the C-O overlap population is further reduced to 1.094 in a c(2x2) pattern, following the well-established trend that two-fold bridge-bonded species have a lower stretching frequency than terminally bonded ones.

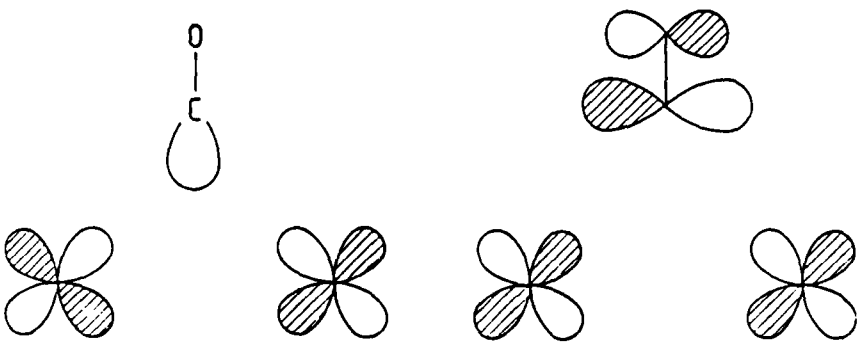

12 13

It is very interesting to note that the 4σ orbitals are also active here. Even more so than in the on-top site; note in the Table 1, the greater depopulation of 4σ for CO bridging.

NO on the Rh(100) Surface

The chemisorption of nitric oxide on transition metal surfaces has many similarities to that of CO, but is more complex due to the additional geometrical possibilities (linear,bent) and the additional electron occupying the $2\pi^*$ orbital. For NO on group VIII transition metals there is evidence for some low temperature dissociative adsorption and a variety of molecular bonding geometries. These include a form with the NO axis tilted away from the surface normal (bent), a bridged form and a linear one. For instance, the bent NO species were found on reconstructed Pt(100)[52] and Ni(111)[53] surfaces. Both bent and linear forms of adsorbed NO were found at room temperature on polycrystalline Ni[30c].

One of the first broad investigations of NO chemisorption was carried out by G. Broden et al[1]. According to the line drawn by these authors, dividing the transition metals into those on which adsorption is strictly molecular and others where dissociation is observed, rhodium (unmarked) is most likely to behave as Ni or Ir, which exhibit both molecular and dissociative NO adsorption. In 1979, Castner et al.[2] reported that NO chemisorption on the Rh(100) occurs with high initial sticking probability at 25°C, forming a c(2x2) LEED structure. These workers stated that thermal NO desorption was complex. In the same year, Campbell and White[37] reported that a polycrystalline

Rh sample at saturation has about 15% of dissociated NO. For some time thereafter, NO chemisorption, especially on the Rh(100), did not receive much attention. Recently, Ho and White[31] reported a low temperature(~100K) adsorption and decomposition study of NO on Rh(100). Adsorption was predominately molecular, with a small dissociative contribution at low coverages, and a saturation coverage of 0.65 ML. The authors suggested that there are two major NO states involved in the chemisorption. The first corresponding to normal molecular adsorption and the second has highly tilted NO molecules, such that both N and O atoms are bound to the surface with a weakened N--O bond. Upon heating the latter decomposed before desorption. Later, Villarrubia, et al.[43] have resolved the vibrational modes of 920 and 1600 cm^{-1} for two such different NO adsorption states at 90K. The lower frequency state was attributed to a highly inclined or side-on (lying down) bonding mode of NO. A higher frequency state of about 1600 cm^{-1}(more accurately at 1590 for low coverages, shifting to 1700 cm^{-1}, at higher coverages) was not unambiguously assignable to a specific adsorption site and geometry. Linearly bonded NO stretching frequencies in transition metal nitrosyls have been observed in this range, although most reported frequencies on single crystal surfaces are slightly higher. On the other hand, several previous assignments of two-fold bridged adsorptions are close to these values, ranging up to around 1600cm^{-1}. Very recently, the same authors[54] reported a broad investigation on NO adsorption, decomposition and desorption on the Rh(100) surface. They verified

the existance of two major NO states, α_1 (lying down) and α_2 (vertically bonded one). Upon heating, 62% of NO decompose, while the the rest desorb molecularly with E_a=28±3 kcal/mol. The α_1 NO decompose with E_a=10.5±0.7 kcal/mol, while the decomposition of vertically bonded α_2 NO is more complex, strongly coverage-dependant, and goes through a lying down α_1 NO state as an intermediate. For a more detailed discussion of this subject see, for example, references 32, 33, 43 and 54.

It appears that for the chemisorption of NO on the Rh(100) surface we do not have enough experimental information to permit an unambiguous assignment of adsorption pattern and geometry. There is although, some evidence that NO should adsorb vertically at two-fold bridging positions, since Villarrubia and Ho[54], in their model to describe NO adsorption on Rh(100), placed vertically bonded α_2 NO in the two-fold bridging sites, and the lying down α_1 NO in the four-fold hollows.For some other Rh surfaces, such as Rh(111), G.B. Fisher and coworkers[32] reported that NO chemisorbs in two-fold bridge sites at all coverages and that NO is partly dissociated at lower coverages (below 0.2 monolayers) with an activation energy for dissociation of 19 kcal/mol. At higher coverages, adsorption is molecular. Therefore, in order to examine adsorption and bonding of linearly bonded NO we performed an extended Hückel calculation for on-top and two-fold bridging geometries, for several coverages ranging from Θ = 1 to Θ = 0.25. The adsorption geometries used were the same as for CO adsorption, as indicated in 3 and 4 and with three different coverages as in 5, 6 and 7. Table 3 chooses again one

Table 3. Some Bonding Characteristics for of On-top and Bridging c(2x2)NO+Rh(100) System, θ= 0.5.

		Free NO	On-top	Bridging
NO Electron Densities	4σ	2	1.85	1.81
	$1\pi_x$	2	1.98	1.96
	$1\pi_y$	2	1.98	1.89
	5σ	2	1.71	1.73
	$2\pi_x$	0.5	1.09	0.86
	$2\pi_y$	0.5	1.09	1.27
Overlap Populations	N-Rh	-	0.72	0.54
	N-O	1.16	0.89	0.91
Binding Energy (eV)[a]		-	2.50	3.24

[a] Binding energy deffined as $(E_{NO} + E_{Rh(100)}) - E_{NO+Rh(100)}$.

typical coverage for a comparison.

NO chemisorption on Ni(111) has been examined earlier by this group[33]. The molecular orbitals of NO are very much like those of CO and, so are the important interactions. Because of the extra electron and the low energy of the NO $2\pi^*$ orbitals, the total filling of the $2\pi^*$ derived orbitals of the composite system is much higher than for CO.

This system is less coverage-dependent than the corresponding CO system. This is indicated by calculations not reported here, in which one observes smaller changes in the N-O overlap populations when going from full to 1/4 coverage. Experimentally, the shift in stretching frequencies in low-high coverage systems is very significant. On the other hand, it seems that our prediction as to which of these two different adsorption geometries is preferred, based on the "binding energies", is in agreement with the experiment, since for Rh(111)[52] and probably Rh(100)[54], the NO adsorption goes exclusively through a bridging geometry. For this geometry our binding energy is considerably stronger.

It is interesting to note that the involvement of 4σ in adsorption, discussed for CO chemisorption, is also present here. The total effect is smaller than in CO, despite the smaller energy separation between the 4σ and 5σ levels. As for CO, this effect is stronger in the case of bridging geometry. The 4σ orbitals are more depopulated in this geometry (Table 3).

The Bending of NO

Since it is difficult, in principle, to resolve experimentally the problem of bridging linear versus terminal bent NO in the NO+Rh(100) system, we wanted to investigate this system theoretically. We also wanted to study the proposed[54,31] multi-step decomposition mechanism of vertically bonded NO, that goes through the NO lying down geometry as an intermediate. A corresponding analysis of the NO+Ni(111) system[33], and of the bonding in discrete nitrosyls[27] was carried out by this group earlier. Thus we emphasize here only the most important features.

There are two likely ways of bending, from an on-top site and from the bridging position. For the sake of simplicity, we did all the calculations for the (2x2) geometry so that the coverage effects while bending are not included.

Bending in the On-top Site

Let us consider bending in an on-top site of NO adsorption, in a (2x2) geometry indicated in the upper drawing in 7. We will assume that the bending takes place in the yz plane as shown in 14 in both perspective and top views. The bending or tilting

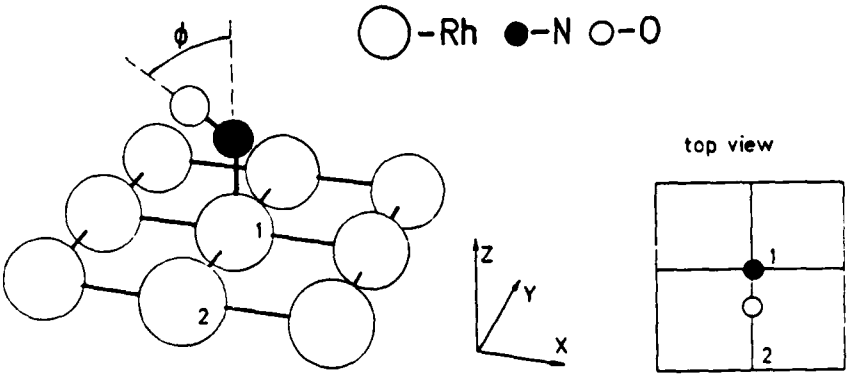

angle ϕ is defined between the surface normal and the direction of N-O bond. In 14 we give the coordinate system that will stay unchanged throughout this paper.

The results of our calculations are shown in Table 4 as a function of bending angle ϕ. As the bending angle increases from 0^0 to 45^0, the N-O overlap population decreases i.e. the NO bond is weakened. The N-Rh overlap population also decreases. The orientation of NO 5σ and 2π orbitals and the d_{yz} and d_{z^2} of the surface Rh are shown in 15 and 16. Upon bending, the orientation of the 5σ orbital enables it to interact with metal yz orbitals, but this interaction is not strong enough to compensate for the loss in 5σ-d_{z^2} interaction (6).

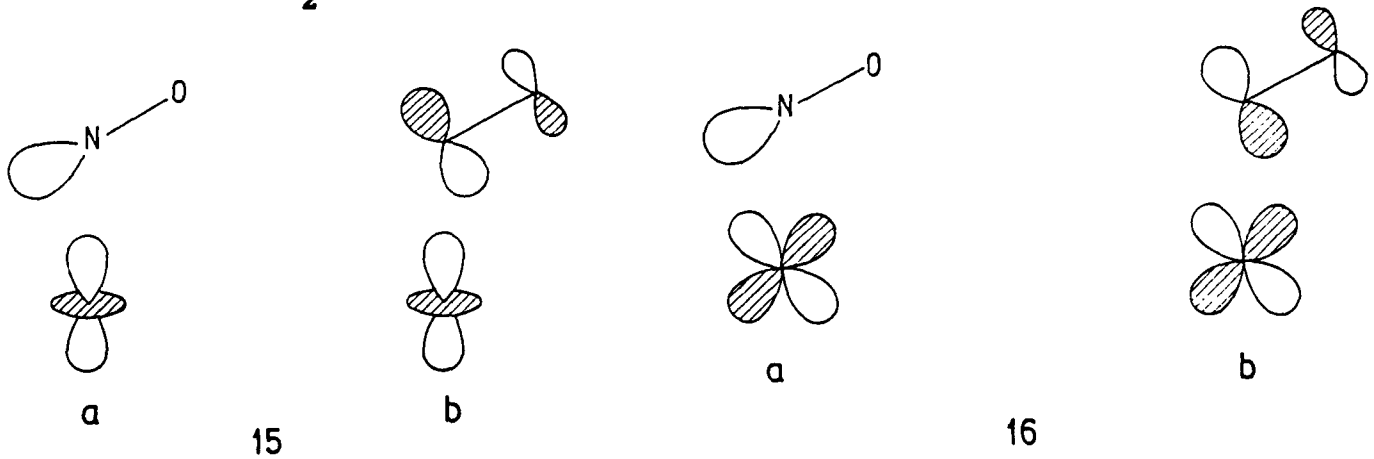

As the NO bends, 4σ and 5σ interact less with the metal. This is why their population moves toward 2.0. The π_y and σ orbitals mix and hybridize, so that $2\pi_y$ (really a mixture of $2\pi_y$ and $2\pi_z$) interacts with more orbitals of the metal, such as d_{z^2}, s and p_z. Therefore, it gains more electron density than the $2\pi_x$ orbital. This increased occupation of antibonding levels is the main reason for weakening of the N-O bond in the bent geometry.

Table 4. Bending of NO in the yz plane (along the surface Rh-Rh bond) in an on-top site (see 14).

	ϕ	0^0	45^0	90^0
NO Electron Densities	4σ	1.85	1.86	1.90
	$1\pi_x$	1.98	1.98	1.97
	$1\pi_{y(z)}$	1.98	1.98	1.90
	5σ	1.71	1.77	1.83
	$2\pi_x$	1.09	1.02	1.37
	$2\pi_{y(z)}$	1.09	1.43	1.09
Overlap Populations	N-O	0.89	0.82	0.85
	N-Rh(1)	0.72	0.64	0.42
	O-Rh(2)	-	0.00	0.12
$d_{O-Rh(2)}$ (A)		4.07	3.30	2.44
Binding Energy (eV)		2.50	2.21	1.52

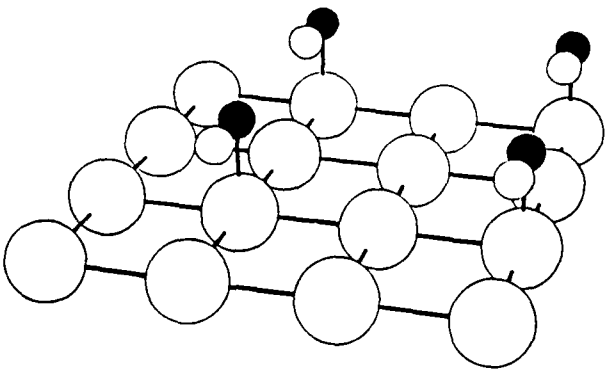

17

By further bending, ϕ=90^0, we reach the situation shown in 17. The NO bond now lies parallel to the Rh(1)-Rh(2) surface bond, with the N atom being exactly on-top of the Rh(1) atom. This geometry is particularly important since some similar states have been detected experimentally. This will be discussed in more detail below, in a section analyzing possible geometries of NO parallel to the surface. Upon this further bending, the N-O overlap population increases somewhat, the N-Rh overlap population decreases further. On the other hand, the O-Rh(2) overlap population grows to the substantial positive value of 0.12 with the relevant atoms being 2.44 A apart. Now we have a very interesting bonding pattern in which the $2\pi_z$ interacts with the surface in the way the 5σ did in the linear geometry, and the 5σ takes over the interaction with the Rh(1) d_{yz} orbitals. The total NO-surface interaction is weaker and the binding energy is reduced to only 1.52 (Table 4). We also studied further bending of NO up to 110^0. The results are not reported in the table but they continue the trend of N-O and N-Rh overlap populations decreasing further. It appears that this bending is not a good candidate for a dissociation mechanism

pathway since the changes in the N-O overlap population do not show the required significant NO bond weakening.

Another possibility for bending in an on-top position is shown in 18. Now the bending is toward a four-fold hollow, i.e. in the diagonal of the xz and yz planes. One is led to consider this variant, as a precursor to N-O dissociation, because it is known that atomic species tend to occupy high symmetry positions such as the four-fold hollow site[55].

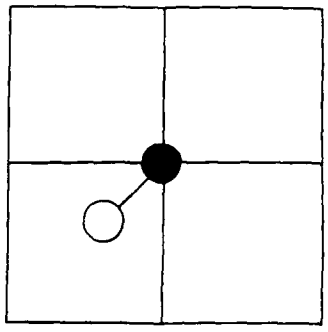

top view

18

What happens in the calculations is that the binding energy decreases steadily and the NO overlap population behaves just as it did for bending "along a bond". So this bending toward a hollow does not look like a good prospect for the dissociative reaction pathway either.

Bending in a Bridging Position

The two bending modes we single out for study are in the yz plane (toward a hollow, 19) and in the xz plane (toward a bond, 20). The first process, bending toward a hollow, does not seem to lead to anything new - once again the NO bond strengthens on 90^{0} bending.

The second bending mode, 20, is more interesting; the

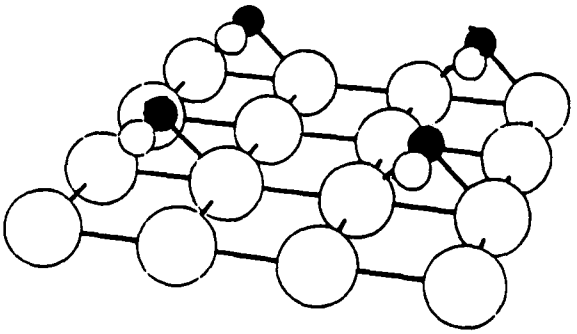

19

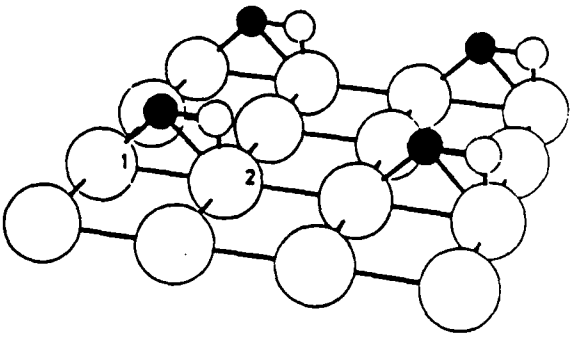

20

computational results for two bending angles are summarized in Table 5. There are two entries for the N-Rh overlap populations since the bending is not symmetrical with respect to the the Rh(1) and Rh(2) surface atoms. As NO bends, the orientation of the σ and π orbitals changes. Among these, the $2\pi_y$ stays essentially the same, but there is a certain drop in the $2\pi_x$ (i.e. $2\pi_{x,z}$ for $\phi=45^0$) electron density. As a result, the N-O overlap population becomes larger. The bending of NO in the x direction reduces the possibility of N-Rh(2) interaction since 5σ is moved away and directed more toward Rh(1). The corresponding overlap population is significantly reduced. The N-Rh(1) overlap population is somewhat increased. The overlap population between oxygen and the Rh(2) atom is still negative so that we still have an antibonding interaction here.

With further bending of NO to 90^0, the situation changes a lot. The 4σ-5σ interactions with the surface Rh(1) and Rh(2) orbitals are increased and both of these orbitals are depopulated. There is a certain increase in 1π orbital

Table 5. Bending of NO in the xz plane while bridging (20).

	ϕ	0^0	45^0	90^0
NO Electron Densities	4σ	1.81	1.83	1.73
	$1\pi_{x(z)}$	1.89	1.87	1.88
	$1\pi_y$	1.96	1.95	1.81
	5σ	1.73	1.75	1.64
	$2\pi_{x(z)}$	1.28	0.95	1.27
	$2\pi_y$	0.87	0.88	0.94
Overlap Populations	N-O	0.91	1.01	0.89
	N-Rh(1)	0.54	0.56	0.49
	N-Rh(2)	0.54	0.32	-0.05
	O-Rh(2)	-	-0.03	0.71
$d_{O-Rh(2)}$ (A)		2.83	2.22	1.37
Binding Energy (eV)		3.21	2.67	3.05

interactions. The $2\pi_y$ orbitals are still almost unchanged, but the $2\pi_x$ (the $2\pi_z$ now) occupancy is getting larger. The $2\pi_z$ interacts in the way the 5σ interacted in the linear case, and is filled as well. The net result of all of this is a significant weakening of the NO bond (note the decrease in the NO overlap population). N-Rh(1) overlap population decreases. There is a very weak antibonding N-Rh(2) interaction, but a large increase in the O-Rh(2) overlap population, occurring mainly through the 4σ and surface d_{xz} interactions. It must be said that the O-Rh(2) distance is much too short at 90^0, so that bonding is overestimated.

The binding energy increases at 90^0 in mode 20, and finally we have found a way to weaken the NO bond. Perhaps this is the way the NO dissociates. But first let's examine a set of alternative geometries.

Lying Down NO

In the preceding discussion, we have mentioned a few different geometries with the NO lying down, i.e. parallel to the surface. Such NO species stable at lower temperatures and coverages, have been observed experimentally on this surface. First, Ho and White[31] proposed an NO adsorption state with a weak NO bond and with both N and O interacting with the surface atoms for several desorption peaks observed in the thermal desorption of NO from Rh(100). Villarrubia, et al.[44,54] recently reported a stable low frequency NO species adsorbed on Rh(100) and assigned it to either a highly inclined structure or one lying parallel to the surface, and proposed a model where lying down NOs are occupying four-fold hollow positions. A similar N_2

adsorbed species have been observed on Fe(111)[56] and on K-promoted Ru(001)[57]. Side-on bonded CO molecules have also been reported on the Cr(110) surface[58]. Such experimental findings have been theoretically considered in the case of CO on the Cr(110) surface by Mehandry and Anderson[15] and in the case of NO on various platinum surfaces by the Masel group[59]. The first have used an atom superposition and electron delocalization MO theory, with the surface represented by a two-layer thick cluster of 33 chromium atoms.

If we begin to study the bonding possibilities for NO lying down on a surface, we are led naturally to consider a set of geometries, 21-28. 21, 22 and 24 have been discussed in the previous section. These include not only the point reached at 90^0 from on-top or bridging linear origins, but other geometries as well.

Some computational results for these geometries are compared in Table 6. Let's discuss them one by one. In 21, obtained by bending from the linear geometry, we lose the N-surface interaction (the N-Rh overlap population gets smaller) and gaining some new oxygen-surface interaction (see Table 4). As we bend NO from linear to lying down position 22, starting in the bridging position, the nitrogen completely loses its bonding interaction with the rhodium atom toward which the NO bends, the oxygen atom comes very close to this Rh atom, acquiring a large positive overlap population (see Table 5). It seems likely that the NO group as a whole will shift, in response to bonding effects, to a geometry such as 23. For this geometry, we have

Table 6. Various possibilities of NO lying parallel to the Rh(100) surface.

Geometry	Overlap Populations			d_{O-Rh}(A)	Binding Energy(eV)
	N-O	N-Rh	O-Rh		
21	0.85	0.42	0.12	2.44	1.52
22	0.89	0.49	0.71	1.37	3.05
23	0.90	0.56	0.39	1.90	2.49
24	0.85	0.40	0.02	2.79	1.39
25	0.98	0.52	0.38	1.90	2.09
26	0.96	0.34	0.07	2.44	0.97
27	0.94	0.47	0.31	1.90	1.93
28	1.00	0.24	0.12	1.90	1.98

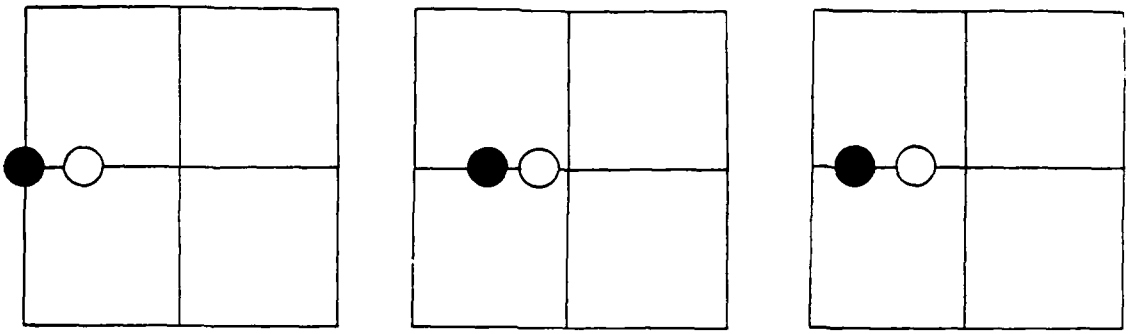

21 22 23

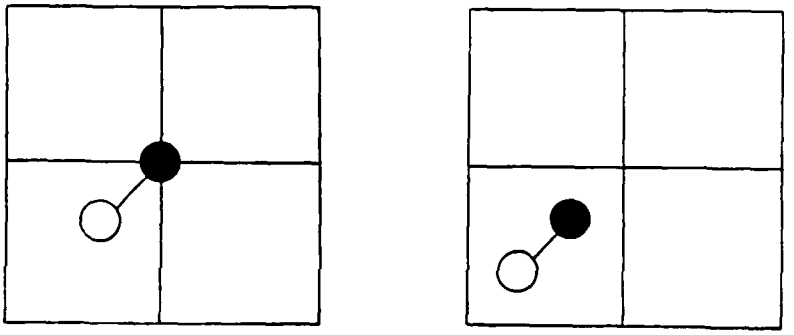

24 25

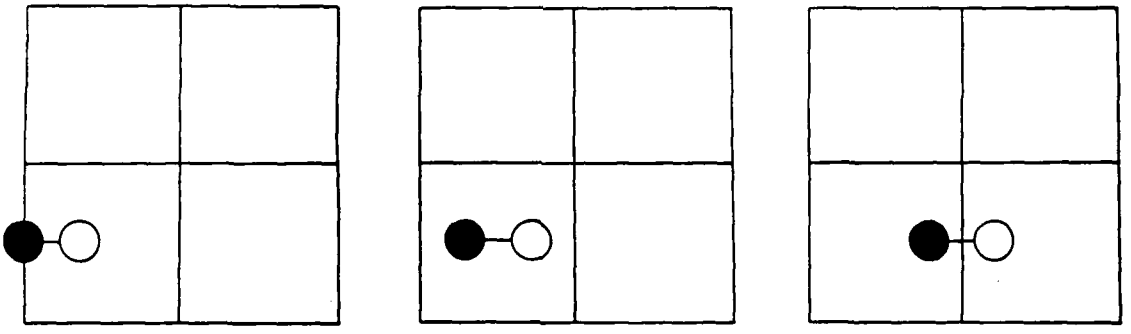

26 27 28

set both N-Rh and O-Rh distances equal to 1.90A and kept the N-O distance at 1.15A, as earlier.

Another bending possibility from an on-top position is toward a four-fold hollow, leading to 24. The bending is also accompanied by a decrease in N-Rh and N-O overlap populations. This bending is not energetically favored, at least not if the position of the N atom is fixed during the bending. One possible change might be to move the N atom along the diagonal of the (100) face, to reach the geometry shown in 25. In this case too, the N-Rh and O-Rh distances are 1.90 A, and the N-O distance is 1.15 A as before.

It is interesting to note here that according to the calculations of Mehandru and Anderson[15], the most stable form of CO adsorbed on Cr(110) is with CO lying across the longer diagonal of the (110) face. Similarly the Masel group[59] has found that there is a good match between the orbitals of the metal and of the adsorbed NO (in the case of Pt(100)) if the NO lies across the diagonal of the unit cell, and concluded that this will lead to NO dissociation. In going from 24 to 25, the $2\pi^*$-surface interaction decreases but all the other NO orbitals are more involved in bonding, especially the 4σ and 5σ. As a consequence of this, the N-O overlap population is much larger in 25 and so are the N-Rh and O-Rh overlap populations. This movement is energetically favored.

Another possible geometry considered for lying down NO originates from bending from the bridging position toward the four-fold hollow 19. The top view of NO lying down in this geometry is shown in 26. During this bending, the binding energy increases continuously, the N-O overlap population increases

after an initial drop at ϕ=45^{0} and the N-Rh overlap population constantly decreases. Since by this bending we are gaining some new attractive O-surface inteactions, one again expects further motion to optimize these interactions. The NO group can move "right" from the position shown in 26 to reach a more symmetrical position,that shown in 27, or it can move "left" to occupy a position where it lies perpendicular to the Rh-Rh surface bond, directly above its midpoint, as shown in 28. In going from 26 to 27, the interaction of 4σ and 5σ with the surface orbitals increases, the 1π orbital's electron densities decrease, while the 2π^{*} increase slightly. As a result of these changes, the N-O overlap population decreases somewhat and overlap populations between oxygen and nitrogen atoms with the surface increase. The N-Rh and O-Rh overlap populations in Table 6 refer to the nearest surface Rh atoms. The changes in these overlap populations lead to a higher binding energy and this movement is energetically favored. The same is true on going from 26 to 28. But the bonding pattern and consequently the NO σ orbitals densities are quite different. The NO σ orbitals do not have a suitable geometry for interaction with the surface atom any more. The overall interaction goes primarily through NO π orbitals, but the total NO 2π^{*} orbital filling is slightly smaller that in 26 and 27, so that the N-O overlap population is higher. Still the total energy change is essentially the same as in 27.

In conclusion we can say that a geometry for highly inclined or lying down NO on the Rh(100) surface, according to our calculations, is likely to be 23, although 25 and 27 should

not be disregarded as possible candidates. It should be noted again that 27 was proposed[54] to be the lying down NO geometry.It is very hard to give a definitive answer to this question using our computational method. The discussion in this section was partly based on energetic arguments. In general we tend to avoid such because of our unwillingness to trust the total energies given by the extended Hückel method.

The Coadsorption of NO and CO

The oxidation of CO and simultaneous reduction of NO over platinum group metal surfaces is of great importance in pollution control since NO is a major pollutant. There have been relatively few mechanistic studies examining the NO/CO process on well-characterized rhodium surfaces, although this metal is the only catalyst which works effectively to reduce NO in automobile exhaust environment.

Campbell and White[37] have examined nitric oxide reduction with carbon monoxide on polycrystalline rhodium wire, using the flash desorption spectroscopy-FDS. They found that adsorbed NO molecules dissociate into adsorbed nitrogen and oxygen. Oxygen reacts with either adsorbed or gas-phase CO to form carbon dioxide. Dubois et al.[5] have reported evidence for an oxygen intermediate in the NO/CO process on the Rh(331) single crystal surface using HREELS and AES and indicated that under their reaction conditions, the formation of gaseous molecular nitrogen is a fast process. Two recent mechanistic studies came from the work of G.B. Fisher[38b,38c,38e] and Hendershot and Hansen[39]. The first studied the reaction on the Rh(111)

surface and concluded that the rate determining step (as well for CO/O_2 reaction) is $CO(a) + O(a) \rightarrow CO_2(gas)$. In recent work[38e] they argued about the possibility of true bimolecular reaction being involved on Rh(111) surface, and that the reaction rate on Rh(100) is significantly different from the one on Rh(111) surface. The second contribution is more interesting for us since it deals with CO/NO processes on the Rh(100) surface. The authors found that this process is selective toward the production of N_2 and a CO_2, but that some other steps must be present in the mechanism, including the formation and decomposition of N_2O and NO_2 adsorbed species. Also, they stated that the NO dissociation, i.e. adsorbed atomic oxygen does not play an important role in the high pressure reactant partial pressure conditions. Villarrubia and Ho[54] also reported a low coverage coadsorption effects of lying down NO with O_2, NO and CO, and concluded that coadsorbates will convert the lying down α_1 NO into a vertically bonded one, with CO being about two times less effective than O_2 and NO.

Now let us investigate the coadsorption of CO and NO on the Rh(100) surface with our calculational tools. The general procedure that we will adopt is to put CO and NO on the surface at the same time in representative positions suggested by experimental studies. By following the trends in orbital electron density and overlap population changes, we can look for indicators of NO bond weakening and CO_2 formation.

There are a large number of possible arrangements of CO and NO on this surface, as both can, in principle, assume bridging

or on-top adsorption sites. Let us first consider the situation where CO and NO are 3.80 A apart (the surface unit cell diagonal). Two possibilities are one with both CO and NO being in bridging positions 29 and one with both in on-top positions 30. The overlayer has a c(2x2) structure in both cases comprised of p(2x2) structures of the individual adsorbates giving a total

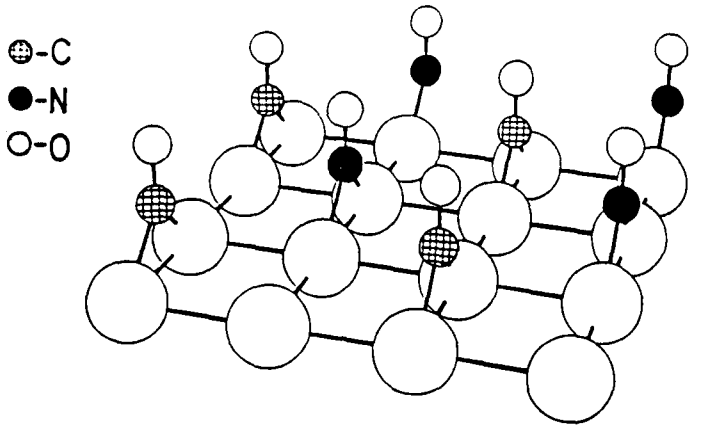

29

coverage of 1/2. The drawings give a perspective view showing only the surface layer of the Rh slab. The big circles represent Rh atoms, while C, N and O atoms are indicated. The coordinate system is the same that was shown in 14.

In these geometries, CO and NO do not "feel" each other very much. The overlap populations and electron densities have not changed significantly from the case of individual adsorption. This is consistent with our previous conclusion that the coadsorbate interactions for both the CO and NO are not significant for distances greater than the van der Waals radii.

For 29 we considered the bending of NO with the bending angle ϕ being defined as before. The bending direction is toward the four-fold hollow, so that C_{CO} and O_{NO} would come closer as

the bending angle approaches 90^{o}.

With bending, the NO and N-Rh overlap populations do not seem to be affected much by the presence of CO, since they are nearly the same as they were in 19. The C-O overlap population increases and the C-Rh overlap population decreases relative to the case of CO adsorption. There is a very weak repulsive interaction between the adsorbates. The differences are small compared to 1/2 coverage adsorption of each individual adsorbate. The origin of this so-called "repulsion" may be competition of the CO and NO for surface electron density.

A similar situation is observed when both CO and NO are in on-top positions 30 with the bending direction of NO being along

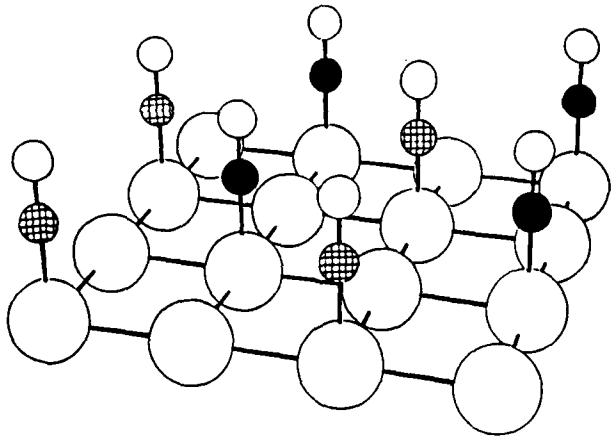

30

the surface Rh-Rh bond.

It is clear that in these geometries with a total coverage of 1/2, CO and NO are too far apart to interact strongly. Therefore, to model the reactivity of CO and NO, these two adsorbates must approach each other in a realistic way. One possibility has the same initial geometry as in 30 but this time the bending is toward the four-fold hollow and, hence, the

oxygen of the NO moves closer to the CO molecule. For a bending angle of 90^{o}, the O_{NO}-C_{CO} distance becomes 2.65A, and the overlap population between them is still negligible. We can see some of the coadsorption effects, but they are still weak. The adsorbates may be too far away for a significant through -space interaction or this geometry may not be suitable for effective orbital interaction. To achieve the values of O-C-O angle in the transition metal complexes of CO_2, the NO bending angle was increased to 110^{o}. No significant changes were produced, however.

Several other possibilities exist which will provide for shorter contacts between the C_{CO} and O_{NO}. These include increasing the total adsorbate coverage or making adjustments in the adlayer structure. The previous discussion was based on an overall c(2x2) pattern comprised of p(2x2) patterns of each adsorbate.

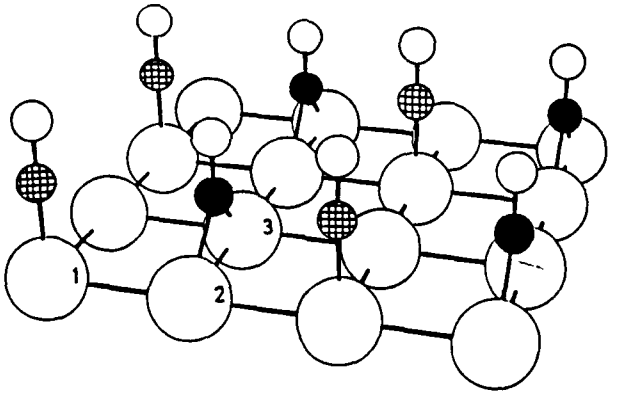

31

We can imagine such a situation where CO is adsorbed on-top and NO in the two-fold bridging position as shown in 31. These are the sites that CO and NO would prefer in the absence of

competing coadsorbate interactions. The results of our calculations, for this geometry are summarized in Table 7. The coadsorption effect for $\phi = 0^0$ is somewhat stronger now, and is reflected in higher C-O and N-O overlap populations. This is consistent with HREELS data showing higher CO and NO stretching frequencies with increasing coverages, i.e., with the presence of repulsive interactions. Some decrease in C-surface and N-surface interaction is expected, but in our calculations, these overlap populations are essentially the same. The N-Rh(3) overlap population is somewhat higher than when NO is adsorbed alone and is suspected to be a consequence of CO-NO repulsion. With further bending, we gain some attractive C-O_{NO} interaction but the repulsive interactions are stronger, so that the C-surface interaction is reduced and C-O overlap population increased. The energetics of these changes show a constant decrease in binding energies, so that we could conclude that this arrangement does not lead to desired changes, either. These coadsorption effects can support the experimental finding of Villarrubia and Ho[54], that lying down NO will be converted into a vertically bonded one when coadsorbed with CO.

Another possible arrangement of coadsorbed CO and NO is shown in 32. Both adsorbates are in bridging positions, but now the overall adsorption geometry gives a 2x1 structure with nearest neighbor coadsorbate interactions of 2.69 A. The NO bending direction is toward the four-fold hollow.

Again when NO is linear there is no significant coadsorption effect. CO shows the same effects whether the nearest neighbor

Table 7. The coadsorption of CO and NO on the Rh(100) surface (31) with the NO bending toward the four-fold hollow.

	ϕ	0^0	45^0	90^0	110^0
CO Electron Densities	5σ	1.67	1.67	1.64	1.65
	$2\pi_x$	0.35	0.36	0.32	0.66[a]
	$2\pi_y$	0.36	0.37	0.34	
NO Electron Densities	5σ	1.72	1.75	1.75	1.79
	$2\pi_{x(z)}$	0.85	0.99	1.04	1.98[a]
	$2\pi_y$	1.27	1.29	1.06	
Overlap Populations	C-O	1.24	1.23	1.25	1.26
	C-Rh(1)	0.86	0.85	0.81	0.83
	N-O	0.92	0.89	0.96	1.00
	N-Rh(3)	0.55	0.50	0.34	0.27
	$C\text{-}O_{NO}$	0.00	0.03	0.05	0.01
Binding Energy (eV)		6.26	5.60	3.43	3.26

[a] The total over two 2π orbitals.

adsorbate is NO or another CO. Of course, things change when NO starts to bend since the C-O_{NO} distance is getting smaller.

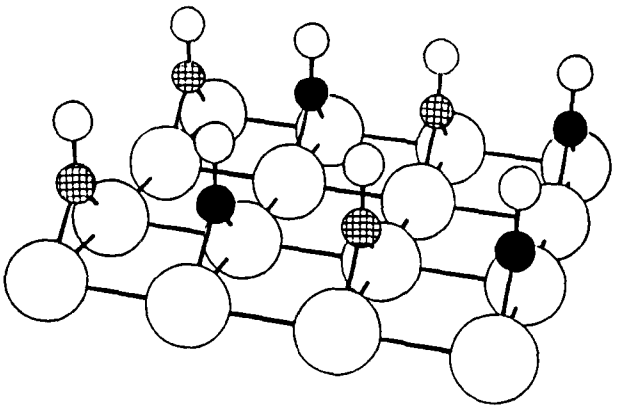

32

For the $\phi = 0^{0}$ the distance between carbon and nitric oxide oxygen is 2.92 A and when NO bends to 45^{0}, it is reduced to 2.02 A. At this distance, we can expect some interaction, and it is reflected in the small positive C-O_{NO} overlap population of 0.02. The C-O and C-Rh overlap populations are reduced. Also, there is a small repulsive interaction between the carbon and nitrogen (a small negative overlap population of -0.02). When NO is lying down, the carbon and nitric oxide oxygen are now only 1.54 A apart and the orientation of the CO π_x and NO 5σ orbitals is suitable for a strong interaction. This results in a large positive C-O_{NO} overlap population of 0.45, compared to the value for a C-O single bond of 0.56. The occupation of the CO $2\pi^*$ orbitals increases and the bond strength decreases. The C-surface interaction is weaker, since the CO $2\pi^*$ orbitals now interact with NO. But, as in the case when NO is lying down alone on the surface, the N-surface interaction is highly reduced and even additional interaction with CO is not strong enough to weaken the NO bond further. A significant bonding interaction is

observed between C_{CO} and O_{NO}, though.

Another possibility of CO and NO coadsorption is shown in 33. Here both CO and NO are in on-top positions on two nearest surface Rh atoms. The CO-NO distances are the same as in previously discussed geometry 32. Again, the NO bending is in the xz plane and the calculations were performed for the three bending angles. The results are summarized in Table 8.

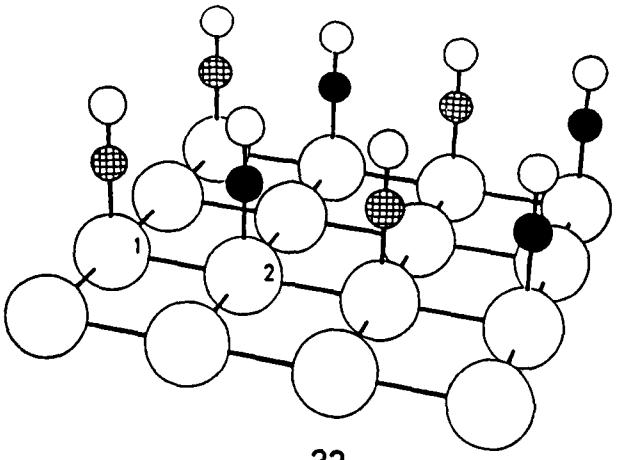

33

This situation is reasonable, as CO prefers on-top geometries on Rh(100), and on the Rh(111) surface NO shifts from two-fold bridging positions to on-top sites when oxygen is present on the surface[32].

Let us first discuss the coadsorption effects for $\phi=0^{0}$ and compare the results to those for individual adsorption of CO and NO. There are no changes in 4σ and 1π orbitals of CO and NO (not shown in the Table). In this geometry, the degeneracy of the $2\pi^{*}$ orbitals is removed and these are considered separately. The CO $2\pi^{*}$ are less populated than for CO on Rh(100) (see Table 1) and, consequently, the C-O overlap population is larger. The

Table 8.The coadsorption of CO and NO on the Rh(100) surface in the on-top positions with NO bending in the xz plane (see 33).

	ϕ	0^0	45^0	90^0	110^0
CO Electron Densities	5σ	1.66	1.67	1.64	1.61
	$2\pi_x$	0.33	0.43	0.73	0.59
	$2\pi_y$	0.35	0.35	0.42	0.38
NO Electron Densities	5σ	1.70	1.72	1.55	1.62
	$2\pi_{x(z)}$	0.99	1.23	0.98	1.02
	$2\pi_y$	0.97	0.98	1.25	1.48
Overlap Populations	C-O	1.24	1.20	1.02	1.12
	C-Rh(1)	0.86	0.87	0.69	0.68
	N-O	0.91	0.87	0.88	0.82
	N-Rh(2)	0.72	0.66	0.42	0.28
	C-N	0.01	-0.03	-0.05	-0.04
	$C-O_{NO}$	0.00	0.04	0.47	0.38
	O_{NO}-Rh(1)	0.00	0.05	-0.03	0.00
Binding Energy (eV)		5.34	3.81	2.50	2.98

same is true for NO (see Table 3). Both the C-Rh and N-Rh overlap populations are smaller. This represents a weaker interaction with the surface and would result in a greater CO or NO stretching frequency.

The coadsorbate interaction is stronger when NO bends to 45^0. The C-O overlap population is significantly reduced due to the C_{CO}-O_{NO} interaction which now has a positive overlap population of 0.04. The N-Rh and C-Rh overlap populations are reduced, but the N-O overlap population is greater than in the case of single NO adsorption. Evidently, these changes are a consequence of overall repulsive interactions.

With further bending of NO to 90^0, the C-O and C-Rh overlap populations are reduced further. The N-O overlap population is somewhat larger and, in fact, greater than when the NO is adsorbed alone in the same geometry (0.66 vs. 0.65). We have significant interaction between carbon and nitric oxide oxygen with an overlap population of 0.47. The C_{CO}-O_{NO} distance is the same as in 32, but here they interact more.

For $\phi=0^0$-90^0, the trend in binding energy is toward weaker adsorption, but with further bending to 110^0, the overall interaction becomes more attractive, with binding energy rising again. The C-O overlap population is somewhat larger but the C-Rh interaction is reduced further. The N-O overlap population is smaller (0.62) than when the NO is alone at the surface in the same position (0.64).

In general, with this bending, we are approaching the situation where there is a tendency for CO_2 formation, but the

energetic changes in these systems are not favorable. We even tried to calculate this system with smaller initial bending angles of 15^0 and 30^0 to investigate the energy changes, but the energy difference of these systems (5.23 and 4.85 eV, respectively) indicate a constant decrease in binding energies with bending.

We can also imagine coadsorption geometries where both the CO and NO are in the bridging positions, being bound to the same surface Rh atom. One of two such possibilities is shown in 34, where CO and NO are bridging mutually perpendicular surface Rh-Rh bonds. Here we can imagine two possible ways of NO bending

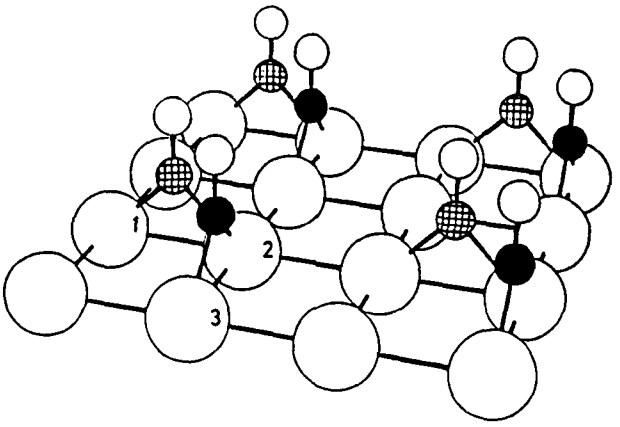

34

in the xz plane and the bending toward the "common" surface atom, i.e. bending in the yz plane. The results are shown in Table 9. The coadsorption effect is the strongest here, since the adsorbates are very close to each other. The carbon and nitrogen are only 1.90 A apart. As in the case of high coverage, both C-O and N-O have larger overlap populations than when they are alone at the surface. The C-surface and N-surface interactions are weakened, with respect to the common Rh(2) atom, while for the other Rh atoms, the overlap populations are slightly larger compared with

Table 9. The coadsorption of CO and NO on the Rh(100) surface (see 34) with NO bending in xz and yz planes.

			xz plane		yz plane	
	ϕ	0^0	45^0	90^0	45^0	90^0
CO Electron Densities	5σ	1.67	1.67	1.67	1.67	1.65
	$2\pi_x$	0.72	0.72	0.64	0.61	0.84
	$2\pi_y$	0.46	0.41	0.86	0.46	0.42
NO Electron Densities	5σ	1.71	1.60	1.76	1.61	1.62
	$2\pi_{x(z)}$	0.87	1.05	1.01	1.00	1.08
	$2\pi_{y(z)}$	1.22	0.98	1.10	0.96	1.21
Overlap Populations	C-O	1.11	0.96	0.91	0.99	1.02
	C-Rh(2)	0.47	0.47	0.36	0.38	0.14
	C-Rh(1)	0.63	0.64	0.50	0.64	0.65
	N-O	0.95	0.91	0.93	0.93	0.84
	N-Rh(2)	0.41	0.40	0.33	0.22	-0.04
	N-Rh(3)	0.55	0.47	0.35	0.48	0.49
	C-N	0.16	0.04	-0.05	0.07	0.01
	$C\text{-}O_{NO}$	-0.08	0.05	0.54	0.04	0.46
	O-O	-0.04	0.28	-0.11	0.25	-0.10
	O_{NO}-Rh(2)	-0.07	-	-	-0.10	0.47
Binding Energy (eV)		4.72	0.79	0.86	-0.30	1.59

the single adsorbate studies. Also, there is a certain C-N attractive interaction which occurs primarily through their π orbitals, including $i\pi$ orbitals. The carbon and nitric oxide oxygen do not interact, since they are, in this geometry, still quite far away from each other(2.28 A).

Let us now discuss the NO bending in the xz plane. For $\phi=45^0$, the C-O and N-O overlap populations are further reduced. While the overall C-surface interaction remains essentially the same, the N-surface interaction is reduced. The weakening of the C-O bond is mainly due to the oxygen-oxygen interaction which presumably goes through the $i\pi$ orbitals (not shown in the Table 9) and some through the NO σ orbitals. We still have some positive C-N overlap populations and a small positive carbon-oxygen (from NO) overlap population of 0.05, as the $C-O_{NO}$ distance is now 1.66 A. When we bend the NO further $\phi=90^0$, this distance is reduced to 1.36 A which results in a high $C-O_{NO}$ interaction with an overlap population of 0.54. The C-O overlap population is reduced to 0.91. The N-O overlap population (0.93) is now larger than for $\phi=45^0$, due to the smaller N-surface interaction, but smaller with respect to NO alone at the surface in the same geometry. This geometry is showing a strong tendency for CO_2 formation and some small effect to reduce the N-O bond strength, but the energetics of these changes do not really favor them.

The bending of NO to 45^0 in the yz plane, toward the surface Rh(2) atom is energetically unfavorable. The trends in overlap population are very similar to those of bending in the xz plane, except for the N-surface overlap populations. They change

logically and the N-Rh(2) overlap population decreases significantly and N-Rh(3) decreases also, though not as much. Both are much smaller than the corresponding values when NO is alone at the surface. When NO is lying down in this arrangement, the carbon and oxygen from NO are again very close to each other (1.36 A), only now the Rh(2) surface atom is "between" them. Again 4σ and 1π CO and NO orbitals are strongly involved in bonding. There is a depopulation of the NO 1π orbitals and a greater donation into the 2π's. Hence, the N-O overlap population is reduced. The C-O overlap population is larger than when $\phi=45^{0}$, but still much lower than when CO is alone at the surface. The N-Rh(2) overlap population is negative and the overlap population between carbon and O_{NO} strongly increases. The CO-surface interaction is further reduced, with C-Rh(2) overlap population of only 0.13, so that the CO is weakly bound to the surface now. If we have a situation in which weakly bound NO species (lying down or highly inclined) at the surface approache coadsorbed COs, in this geometry, then CO_2 and N species are possible products, with CO_2 being weakly bound to the surface.

Finally, we suggest a possible geometry where both CO and NO are in bridging position and bound to adjacent Rh atoms as shown in 35. The bending of NO is in the xz plane here, toward the Rh(2) atom. The results are given in Table 10.

The coadsorption effect is not strong (for $\phi=0^{0}$) but notable. The occupation of the CO $2\pi^{*}$ orbitals is larger than when CO is alone at the surface (see Table 1), but the CO overlap

Table 10. CO and NO coadsorbed on the Rh(100) surface in the geometry shown in 35, with NO bending in the xz plane.

	ϕ	0^0	45^0	90^0
CO Electron Densities	5σ	1.68	1.66	1.65
	$2\pi_x$	0.77	0.74	0.70
	$2\pi_y$	0.44	0.45	0.42
NO Electron Densities	5σ	1.72	1.72	1.44
	$2\pi_{x(z)}$	1.23	0.73	1.32
	$2\pi_y$	0.81	0.93	0.96
Overlap Populations	C-O	1.10	1.10	1.08
	C-Rh(2)	0.62	0.54	0.26
	C-Rh(1)	0.62	0.61	0.62
	N-O	0.94	1.06	0.85
	N-Rh(2)	0.54	0.31	-0.02
	N-Rh(3)	0.54	0.53	0.45
	C-N	0.01	-0.02	-0.03
	$C-O_{NO}$	0.00	0.02	0.33
	O-O	0.00	-0.08	-0.10
	O_{NO}-Rh(2)	-0.08	-0.09	0.56
Binding Energy (eV)		4.98	5.53	4.82

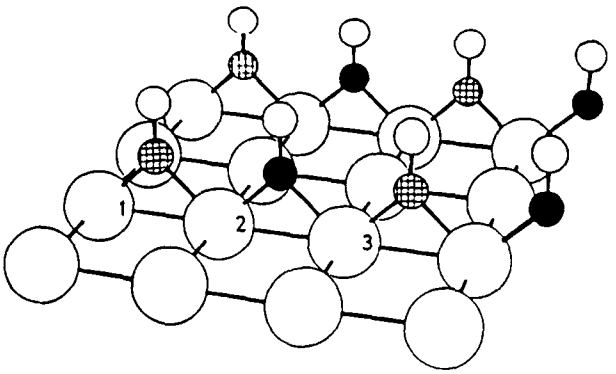

population is somewhat larger. This is due to a weaker CO-surface interaction. The same is true for NO (see Table 3). Again, this is consistent with the experiments which suggest that at high coverages, the stretching frequencies shift to a larger values and the desorption temperatures decrease.

For the bending angle of 45^{O}, both CO- and NO- surface interactions are reduced. This effect is greater for NO and is reflected in a lower occupation of the $2\pi^{*}$ orbitals and larger N-O overlap population. We cannot see significant interaction of the oxygen from NO with the carbon and Rh(2) atoms,even though the distances of 2.04 and 2.22 A, respectively, suggest that some interaction might occur. When NO is lying down, these distances are reduced to 1.54 and 1.36 A, respectively. The CO-surface interaction is reduced and the nitrogen loses its interaction with the surface Rh(2) atom. The N-surface interaction here is smaller than in the case of individual NO adsorption. The N-O overlap population is strongly reduced and is smaller than when NO is alone at the surface in the same geometry (0.89-Table 5). As it was proposed earlier, this may be a candidate for the NO dissociation mechanism. C-O overlap population is also further reduced. The oxygen-oxygen overlap population is

negative and oxygen from NO is now more weakly bound to the Rh(2) atom than in the case of individual NO adsorption (0.71-Table 5). CO can interact with lying down NO species at the surface in this geometry, the trends for CO_2 formation and N-O bond breaking are evident.

To conclude this section we can point out that most of the NO bending mechanisms do not favor the CO/NO reaction, but that there are several arrangements, with NO lying down at the surface, which would lead to N-O bond braking and CO_2 formation. So, perhaps, we do not need the NO dissociation as a necessary precondition fo this reaction to occur. In that sense we could support the conclusion of Hendershot and Hansen[39] that the NO dissociation is not important under their reaction conditions. On the other hand we find the strongest effects if NO is lying down along the bridged surface Rh-Rh bond (as in 34 and 35), i.e. the only possible candidate for NO dissociation mechanism in the frame of our bending scheme. But, we were able to produce the desired trends, though to a smaller extent, in some other geometries, as in 34 when NO is lying down with the oxygen being close to a four-fold hollow site (as in 26), or even in 33 with the bending angle greater than 90^0.

Coadsorption of CO and Oxygen

Up to now in all the coadsorption geometries, we applied the bending model for NO dissociation. We have found several geometries of lying-down NO with which the CO could readily react to form CO_2. Now we would like to briefly investigate the

coadsorption of CO and oxygen as the interaction of such species is suggested to be the rate determining step for the CO/NO reaction on Rh(111). The adsorption of oxygen on Rh surfaces has been investigated experimentally[2,55,61]. On the Rh(100) surface[55] oxygen is dissociatively adsorbed in three β states, and there is a low temperature molecular adsorption state. Here we assumed that O_2 has dissociated and that the oxygen are found in four-fold hollow sites. The Rh-O distance of 2.05 A was taken from the corundum structure of Rh_2O_3 system[62].

Keeping the oxygen in the four-fold hollow we have two possible ways to obtain close C(O)-O contact. The first is an on-top sites as in 36, and the second is with CO in the two-fold bridging position, 37. The C-O(ads.) distances are 2.29 A and 1.53 A, respectively.The results for these sites are presented in Table 11.

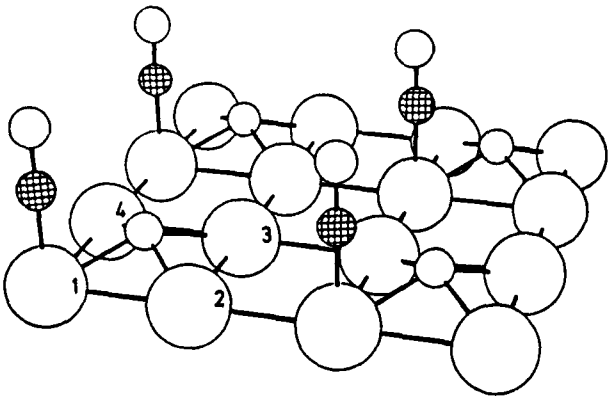

36

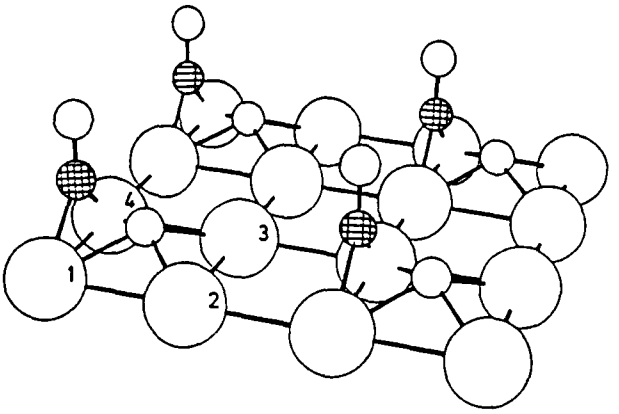

37

Let us first discuss the geometry where the CO is on-top, 36. When coadsorbed with the oxygen, the degeneracy of CO π orbitals

Table 11. The coadsorption of CO and O on the Rh(100) surface in the geometries shown in 36 and 37.

		36	CO or O alone[a]	37	CO or O alone[a]
CO Electron Densities	5σ	1.78	1.78	1.61	1.72
	$1\pi_x$	1.99	1.99	1.90	1.98
	$1\pi_y$	1.99	1.99	1.95	1.95
	5σ	1.64	1.67	1.58	1.69
	$2\pi_x$	0.32	0.36	0.61	0.47
	$2\pi_y$	0.32	0.36	0.73	0.74
O electron densities	s	1.79	1.78	1.72	1.78
	P_x	1.46	1.49	1.30	1.49
	P_y	1.48	1.49	1.45	1.49
	P_z	1.92	1.92	1.75	1.92
Overlap Populations	C-O	1.26	1.23	1.04	1.10
	C-Rh(1)	0.82	0.86	0.44	0.62
	O_a-Rh(1)	0.20	0.23	0.12	0.23
	O_a-Rh(2)	0.23	0.23	0.24	0.23
	C-O_a	0.01	-	0.47	-

[a] CO in on-top or bridging sitees, singly adsorbed in a p(2x2) structure; O in four-fold hollow site, singly adsorbed in a p(2x2) structure.

is removed, but the differences between these orbitals are small. Also, the oxygen p_x and p_y orbitals lose their degeneracy and that effect is slightly greater. CO $2\pi^*$ and 5σ orbitals are somewhat depopulated when compared with CO being alone at the surface. The same is true for oxygen p_x and p_y atomic orbitals. The C-O overlap population increases. This geometry does not provide for efficient C-O(ads.) interaction as the C-O distance is prohibitively long. Instead, we see repulsive interaction of coadsorbates and weaker adsorbate surface bonding.

In the case where CO is in the bridging position, the coadsorbates are closer to each other, and CO π and oxygen p orbitals are colinear, so it is logical to expect more interaction. Indeed, the changes in electron densities and overlap populations are much greater than in the previous case. The C-O overlap population is reduced and we gain a positive C-O(ads.) overlap population of 0.46. At the same time the C-Rh(1) overlap population is reduced as are the overlap populations between the adsorbed oxygen and surface rhodium. The geometry looks promising for the formation of CO_2 molecules at the surface and subsequent desorption as well.

Acknowledgement We thank M. Zonnevylle, R. Wheeler and W. Tremel for helpful discussions during the course of this work and R. Keneski for execution of drawings. Our work was generously supported by the Office of Naval Research.

Appendix

In this paper, all performed computations are tight-binding band calculations of the extended Hückel type. The H_{ii}'s for rhodium were obtained by charge iteration on the bulk metal (with the experimental fcc geometry) using Gray's equation[63], with A, B and C parameters taken from Ref. 64. The carbon H_{ii}'s were taken from an earlier work of this group[12] and were in good agreement with iterated values. The oxygen H_{ii}'s were obtained by charge iteration on CO adsorbed on both sides of the rhodium three-layer slab, keeping the C and Rh H_{ii}'s constant, with the low coverage of 0.25 on both sides to avoid the adsorbate interactions. Nitrogen H_{ii}'s were obtained for NO adsorbed in the same way as CO, with the same procedure, with oxygen and rhodium parameters being constant. Oxygen parameters were previously determined parameters from CO adsorption. B and C iteration parameters for C, N and O atoms were taken from Ref. 65. Extended Hückel parameters for all atoms used, are listed in Table 12.

All the results listed in this paper are from the single-face adsorption calculations, using the three-layer slab model. The geometrical parameters for coadsorption are: C-O, 1.15; N-O, 1.15; Rh-Rh, 2.6893; Rh-C, 1.90; Rh-N, 1.90; and Rh-O, 2.05 (all values in A). The k-point sets varied from 49 to 12 points in order to keep the total number of states for each geometry similar.

Table 12. Extended Hückel parameters.

Orbital	H_{ii} (eV)	ζ_1	ζ_2	c_1[a]	c_2[a]
Rh 5s	-7.31	2.13			
Rh 5p	-3.39	2.10			
Rh 4d	-10.35	4.29	1.97	0.5807	0.5685
C 2s	-18.20	1.63			
C 2p	-9.50	1.63			
N 2s	-23.95	1.95			
N 2p	-10.95	1.95			
O 2s	-27.61	2.28			
O 2p	-11.01	2.28			

[a] Contraction parameters used in the double-ζ expansion.

References

1. G. Broden, T.N. Rhodin, C. Bruckner, B. Benbow and Z. Hurych, Surf. Sci. 1976, 59, 593.
2. D.G. Castner, B.A. Sexton and G.A. Somorjai, Surf. Sci. 1978, 71, 519.
3. L.H. Dubois and G.A. Somorjai, Surf. Sci. 1980, 91, 514.
4. R.J. Baird, R.C. Ku and P. Wynblatt, Surf. Sci. 1980, 97, 346.
5. L.H. Dubois, P.K. Hansma and G.A. Somorjai, J. Catal. 1980, 65, 318.
6. L.A. DeLouise, E.J. White and N. Winograd, Surf. Sci. 1984, 147, 252.
7. E.W. Plummer, C.T. Chen, W.K. Ford, W. Eberhardt, R.P. Messmer and H.-J. Freund, Surf. Sci. 1985, 158, 58.
8. M.W. Lesley and L.D. Schmidt, Surf. Sci. 1985, 155, 215.
9. F.P. Netzer, J.U. Mack, E. Bartel and J.A.D. Matthew, Surf. Sci. 1985, 160, L509.
10. S. Ishi, Y. Ohno and B. Viswanathan, Surf. Sci. 1985, 161, 349.
11. A.B. Anderson and R. Hoffmann, J. Chem. Phys. 1974, 61, 4545.
12. S.-S. Sung and R. Hoffmann, J. Am. Chem. Soc. 1985, 107, 578.
13. A.B. Anderson and Md.K. Awad, J. Am. Chem. Soc. 1985, 107, 7854.
14. P.-L. Cao, Y. Wu, Y.-Q. Chen and D.-J. Zheng, Appl. Surf. Sci. 1985, 22/23, 452.
15. S.P. Mehandru and A.B. Anderson, Surf. Sci. 1986, 169, L281.
16. J. Andzelm and D.R. Salahub, Int. J. Quant. Chem. 1986, XXIX, 1091.

17. G.A. Somorjai, "Chemistry in Two Dimensions: Surfaces"; Cornell Univ. Press: Ithaca and London, 1981; p. 280.

18. G. Blyholder, J. Phys. Chem. 1964, 68, 2772; G. Doyen and G. Ertl, Surf. Sci. 1974, 43, 197.

19. a) R. Miranda, K. Wandelt, D. Rieger and D. Schnell, Surf. Sci. 1984, 139, 430.

b) K. Horn, A.M. Bradshaw, K. Hermann and I. Batra, Solid State Commun. 1979, 31. 257.

c) E.W. Plummer and W. Eberhardt, Adv. Chem. Phys. 1982, 49, 533.

d) F. Grevter, D. Heskett, E.W. Plummer and H.J. Freund, Phys. Rev. B 1983, 27, 7117.

e) G. Loubriel and E.W. Plummer, Chem. Phys. Lett. 1979, 64, 234.

f) R.V. Kasowski, T. Rhodin and M.-H. Tsai, Appl. Phys. 1986, A41, 61; R.V. Kasowski, M.-H. Tsai, T. Rhodin and D.D. Chambliss, Phys. Rev. 1986, B34, 2666; R.V. Kasowski, M.-H. Tsai, T.N. Rhodin and D.D. Chambliss, Sol. State Comm. 1986, 59, 57; R.S. Kasowski, T.N. Rhodin and M.-H. Tsai, to be published.

20. H. Arai and H. Tominga, J. Catal. 1976, 43, 131.

21. H. Conrad, R. Scala, W. Stenzel and R. Unwin, Surf. Sci. 1984, 145, 1.

22. E. Umbach, S. Kulkarni, P. Feulner and D. Menzel, Surf. Sci. 1979, 88, 65.

23. A.A. Chin and A.T. Bell, J. Phys. Chem. 1983, 87, 3700.

24. L.A. DeLouise and N. Winograd, Surf. Sci. 1985, 154, 79.

25. L.A. DeLouise and N. Winograd, Surf. Sci. 1985, 159, 199.

26. R. Eisenberg and C.D. Meyer, Acc. Chem. Res. 1975, 8, 26.

27. R. Hoffmann, M.M.L. Chen, M. Elian, A.R. Rossi and D.M.P. Mingos, Inorg. Chem. 1974, 13, 2666.

28. J.H. Enemark and R.D. Feltham, Coord. Chem. Rev. 1974, 13, 339.

29. R. Hoffmann, M.M.L. Chen and D.L. Thorn, Inorg. Chem. 1977, 16, 503.

30. a) H.P. Bonzel and G. Pirug, Surf. Sci. 1977, 62, 45.

b) G. Pirug, H.P. Bonzel, H. Hopster and H. Ibach, J. Chem. Phys. 1979, 71, 593.

c) A.F. Carley, S. Rassias, M.W. Roberts and T.-H. Wang, Surf. Sci. 1979, 84, L227.

31. a) P. Ho and J.M. White, Surf. Sci. 1984, 137, 103.

b) P. Ho and J.M. White, Surf. Sci. 1984, 137, 117.

32. G.B. Fisher, GM Research Reporet No. PC-289, 1985.

33. S.-S. Sung, R. Hoffmann and P.A. Thiel, J. Phys. Chem. 1986, 90,1380.

34. R.L. Klein, S. Schwartz and L.D. Schmidt, J. Phys. Chem. 1985, 89, 4908.

35. R.J. Gorte and L.D. Schmidt, Surf. Sci. 1981, 111, 260.

36. P.A. Thiel, W.H. Weinberg and J.T. Yates, J. Chem. Phys. 1979, 71, 1643.

37. C.T. Campbell and J.M. White, Appl. Surf. Sci. 1978, 1, 347.

38. a) T.W. Root, L.D. Schmidt and G.B. Fisher, Surf. Sci. 1983, 134, 30.

b) T.W. Root, L.D. Schmidt and G.B. Fisher, Surf. Sci. 1985, 150, 173.

c) G.B. Fisher, GM Research Report No. PC-295, 1986.

d) S.H. Oh, G.B. Fisher, J.E. Carpenter and D.W. Goodman, GM Research Publication GMR-5022, 1985.

e) S.C. Schwartz, G.B. Fisher and L.D. Schmidt, J. Phys. Chem. 1988, 92, 389.

39. R.E. Hendershot and R.S. Hansen, J. Catal. 1986, 98, 150.

40. V.A. Matyshak, M.M. Slinako, R.A. Gazarov, V.I. Panchishnyi, A.A. Kadushin and O.V. Krylov, Kinetika y Kataliz 1986,

XXVII, 167 (Russ.).

41. V. Rives-Arnau and G. Munvera, Appl. Surf. Sci. 1980, 6, 122.

42. a) R. Hoffmann, J. Chem. Phys. 1963, 39, 1397; R. Hoffmann and W.M. Lipscomb, ibid. 1962, 36, 2176; ibid. 1962, 37, 2872.

    b) J.H. Ammeter, H. Bürgi, J.C. Thibeault and R. Hoffmann, J. Am. Chem. Soc. 1978, 100, 3686.

43. J.S. Villarrubia, L.J. Richter, B.A. Gurney and W. Ho, J. Vacuum Sci. Techn. A 1986, 4, 1487.

44. J. Donohue, "The Structure of the Elements"; R.E. Kreiger Publ. Comp., Inc.: Malabar, Florida, 1982; p. 215.

45. M.C. Zonnevylle and R. Hoffmann, Langmuir 1987, 3, 452.

46. J.-Y. Saillard and R. Hoffmann, J. Am. Chem. Soc. 1984, 107, 2006.

47. a) Y. Kim, H.C. Peebles and J.M. White, Surf. Sci. 1982, 114, 363.

    b) D.E. Peebles, H.C. Peebles and J.M. White, Surf. Sci. 1984, 136, 463.

48. C.W. Tucker, Jr., J. Appl. Phys. 1966, 37, 3013.

49. a) W.L. Jorgensen and L. Salem, "The Organic Chemist's Book of Orbitals"; Academic Press: New York, 1973, pp. 78,80.

    b) W.M. Huo, J. Chem. Phys. 1964, 43, 624; A.D. MacLean and M. Yoshimine, IBM J. Res. Dev. Suppl. 1968, 3, 206.

50. T. Hughbanks and R. Hoffmann, J. Am. Chem. Soc. 1983, 105, 1150.

51. R. Hoffmann, J. Chem. Phys. 1963, 39, 1397.

52. M. Ibach and S. Lehwald, Surf. Sci. 1978, 76, 1.

53. S. Lehwald, J.T. Yates, Jr. and M. Ibach, in Proc. IVC-8, ICSS-4, ECOSS-3, Cannes, 1980, eb. by D.A. Degres and M. Costa, p. 221.

54. J.S. Villarrubia and W. Ho, J. Chem. Phys. 1987, 87, 750.

55. G.B. Fisher and S.J. Schmieg, J. Vacuum Sci. Techn. A 1983, 1, 1064.

56. M. Grunze, M. Golze, W. Hirshwald, H.-J. Freund, H. Pulm, U. Weip, M.C. Tsai, G. Ertl and J. Kuppers, Phys. Rev. Lett. 1984, 53, 850.

57. F.M. Hoffmann and R.A. de Paola, Phys. Rev. Lett. 1984, 52, 1697.

58. a) N.D. Shinn and T.E. Madey, Phys. Rev. Lett. 1984, 53, 2481.

b) N.D. Shinn and T.E. Madey, J. Vacuum Sci. Techn. A 1985, 3, 1673.

59. W.F. Banholzer, Y.O. Park, K.M. Mak and R.I. Masel, Surf. Sci. 1983, 128, 176.

60. a) R. Alvarez, E. Cormona, J.M. Marin, M.L. Poveda, E. Gutiérrez-Puebla and A. Monge, J. Am. Chem. Soc. 1986, 108, 2286.

b) M. Aresta, C.F. Nobile, V.G. Albano, E. Formi and M. Manassero, J. Chem. Soc. Chem. Comm. 1975, 636.

c) G. Fachinetti, C. Floriani and P.F. Zanazzi, J. Am. Chem. Soc. 1978, 100, 7405.

61. a) D.G. Castner and G.A. Somorjai, Surf. Sci. 1979, 83, 60.

b) P.A. Thiel, Y.T. Yates and W.H. Weinberg, Surf. Sci. 1979, 82, 22.

c) C.T. Campbell and J.M. White, J. Catal. 1978. 54, 289.

62. J.B.M. Coey, Acta Crysalogr. 1970, B26, 1876.

63. C.J. Ballhausen and H.B. Gray, "Molecular Orbital Theory"; W.A. Benjamin, New York, 1965; p. 125.

64. R. Munita and J.R. Letelier, Theor. Chim. Acta 1981, 58, 167.

65. S.P. McGlyn, L.G. Vanquickenborne, M. Kinoshita and D.G. Carroll, "Introduction to Applied Quantum Chemistry"; Holt, Rinehart and Winston, Inc.: New York, 1964; p.p. 423-431.